Design and Control of Converters for Solar Water Pumping Application

A DISSERTATION

SUBMITTED IN PARTIAL FULFILLMENT OF THE REQUIREMENTS
FOR THE AWARD OF THE DEGREE
OF

MASTER OF TECHNOLOGY
IN
Control & Instrumentation

Submitted by:

SHALINI

2K19/C&I/06

Under the supervision of

Mr. Himanshu Singh

DEPARTMENT OF ELECTRICAL ENGINEERING
DELHI TECHNOLOGICAL UNIVERSITY
(Formerly Delhi College of Engineering)
Bawana Road, Delhi-110042

AUGUST, 2021

DESIGN AND CONTROL OF CONVERTERS FOR SOLAR WATER PUMPING APPLICATION

DELHI TECHNOLOGICAL UNIVERSITY
(Formerly Delhi College of Engineering)
Bawana Road, Delhi-110042

CANDIDATE'S DECLARATION

I, Shalini, Roll No. 2K19/C&I/06, student of M.Tech. (Control & Instrumentation), hereby declare that the project Dissertation titled "Design and Control of Converters for Solar Water Pumping Application" which is submitted by me to the Department of Electrical Engineering, Delhi Technological University, Delhi in partial fulfillment of the requirement for the award of the degree of Master of Technology, is original and not copied from any source without proper citation.

This work has not previously formed the basis for the award of any Degree, Diploma Associateship, Fellowship or other similar title or recognition.

Place: Faridabad **SHALINI**

Date: 10/08/2021

DELHI TECHNOLOGICAL UNIVERSITY
(Formerly Delhi College of Engineering)
Bawana Road, Delhi-110042

CERTIFICATE

I hereby certify that the Project Dissertation titled "Design and Control of Converters for Solar Water Pumping Application" which is submitted by SHALINI, Roll No. 2K19/ C&I/06 [Department of Electrical Engineering], Delhi Technological University, Delhi in partial fulfillment of the requirement for the award of the degree of Master of Technology, is a record of the project work carried out by the student under my supervision. To the best of my knowledge this work has not been submitted in part or full for any Degree or Diploma to this University or elsewhere.

Place: Delhi
Date: 10/08/2021

Himanshu Singh
SUPERVISOR
Assistant Professor
Department of Electrical Engineering
Delhi Technological University

ABSTRACT

This thesis presents designing and modelling of water pumping system powered by solar energy and comprising of BLDC motor drive. It manifests the performance comparison between Zeta, Sepic and Cuk converter based output conditioning of SPV array as well. As the solar insolation level is not constant, SPV array output is controlled using Maximum Power Point Tracking (MPPT) along DC-DC converter in order to ensure maximum power usage from SPV array. MPPT is implemented using Incremental Conductance (INC) algorithm along with Zeta, Sepic and Cuk converters to power BLDC motor drive. The DC-DC converters along with the entire simulation are analyzed for peak insolation level as well as varying insolation level and comparison has been performed on the basis of performance characteristics. The BLDC motor is fed using a six-pulse converter which is controlled using Space Vector Pulse Width Modulation (SVPWM) technique which facilitate maximization of efficiency of whole system. The simulation results are obtained from model created in MATLAB (Simulink) environment.

ACKNOWLEDGEMENT

I am highly grateful to the Department of Electrical Engineering, Delhi Technological University (DTU) for providing this opportunity to carry out this project work.

The constant guidance and encouragement received from my supervisor Assistant Prof. Himanshu Singh of Department of Electrical Engineering, DTU, has been of great help in carrying my present work and is acknowledged with reverential thanks.

I would like to thank Asst. Prof. Himanshu sir for his guidance and continuous support in completion of this project work.

Finally, I would like to express gratitude to all the faculty members of Electrical Engineering Department, DTU for their intellectual support in my M.Tech. study at DTU.

SHALINI

2K19/C&I/06
M. Tech. (Control & Instrumentation)
Delhi Technological University

CONTENTS

LIST OF FIGURES

LIST OF TABLES

ABBREVIATIONS

S. No.	Abbreviation	Description
1	BLDC	Brush less direct current
2	INC	Incremental conductance
3	PMSM	Permanent magnet synchronous machine
4	SVPWM	Space vector pulse width modulation
5	SPV	Solar photo voltaic
6	PWM	Pulse width modulation
7	EMF	Electro motive force

LIST OF SYMBOLS

S. No.	**Solar photovoltaic array**	**Symbol**
1	SPV panel voltage at maximum power	V_m
2	SPV panel current at maximum power	I_m
3	SPV array voltage at maximum power	V_{mpp}
4	SPV array current at maximum power	I_{mpp}
5	SPV array maximum power	P_{mpp}
6	SPV panel open circuit voltage	V_{oc}
7	SPV panel open circuit current	I_{sc}
8	Total SPV panels connected in series	N_s
9	Total SPV panels connected in parallel	N_p

S. No.	**BLDC motor**	**Symbol**
1	Rated power	P
2	Rated speed	N_r
3	Rated torque	T_m
4	Rated Voltage/ DC link voltage	V_{dc}
5	Rated current	I_{dc}
6	Number of poles	N_p
7	Moment of inertia	J
8	Voltage constant	K_e
9	Torque constant	K_t
10	Stator phase resistance	R_s
11	Stator phase inductance	L_s

S. No.	**Power electronics converter**	**Symbol**
1	Duty ratio	D
2	Input inductor	L_1
3	Output inductor	L_2
4	Capacitor	C_1
5	Switching frequency	f_s
6	L_1 inductor current ripple	ΔI_{L1}
7	L_2 inductor current ripple	ΔI_{L2}
8	C_1 capacitor voltage ripple	ΔV_{C1}
9	DC link voltage ripple	ΔV_{dc}

CHAPTER 1: INTRODUCTION

1.1. INTRODUCTION

Solar radiation is a clean source of energy that is available all across the world. It is easy to harness with high efficiency SPV panels available these days and the cost of setup is also decreasing rapidly [1]. All these advantages make it an excellent alternative to conventional energy sources. Also, SPV assembly can be installed remotely with minimum requirements anywhere in the world. Solar energy can be used with all the things that run on electricity, and hence, it becomes an obvious choice for a remote water pumping setup which uses electric motor to rotate turbine [2]. Such water pumping solutions find huge application in farming sector in developing countries where electricity is far from reach and reasonably priced irrigation equipment is not available. Conventional induction motor is now being surpassed by BLDC motor in terms of cost [1]. BLDC motor offers excellent speed control along with reliable and efficient performance [3]. Thus, BLDC motor becomes obvious choice for driving a water pumping system powered by solar energy.

1.2. SOLAR WATER PUMPING SYSTEM

Solar powered water pumping system has SPV array [4] and BLDC motor [5] at its core but it requires various control mechanisms as well in order to achieve control over various aspects of the system. For a remote pumping system, various speeds may be required by the user depending upon the application, hence, speed control for BLDC motor is essential. Field oriented speed control is a well-known speed control method that provides efficient and accurate speed control for BLDC motor. SPV array output is not constant due to varying weather conditions which translates to varying point of maximum power for SPV array. Thus, power extraction mechanism such as MPPT algorithm [6] is required to make sure that operation point is always the point of maximum power. The techniques used to achieve these controls are discussed in next section.

1.3. SYSTEM DESIGN AND CONFIGURATION

The solar water pumping system uses a 3.2kW SPV array which is capable of powering a 2.82kW BLDC motor and supply all the necessary losses. The 3.2kW output of SPV array is obtained at a 1000W/m^2 of peak insolation [7]. SPV array produced output conditioning is done using DC-DC converter along with MPPT module to generate PWM signal [8] that facilitate maximum power transfer. Zeta, Cuk and Sepic converters [9, 10, 11] are the three DC-DC converters used for testing with same simulated environment. MPPT is done using INC algorithm [12] to extract maximum power. The DC link voltage at peak insolation of 1000W/m^2 is 200V. C_2 is DC link capacitor which is equipped to condition the output from DC-DC converter. The six-pulse converter [13] is fed using DC-DC converter output which gives three phase output to drive BLDC motor. SVPWM technique [14] takes shaft angle as feedback from BLDC motor in order to achieve speed control and ensure efficient operation of the motor. The motor shaft is connected to a turbine for pumping application. The parameters and selected values of BLDC motor and SPV array are shown in appendices.

1.4. BLOCK DIAGRAM

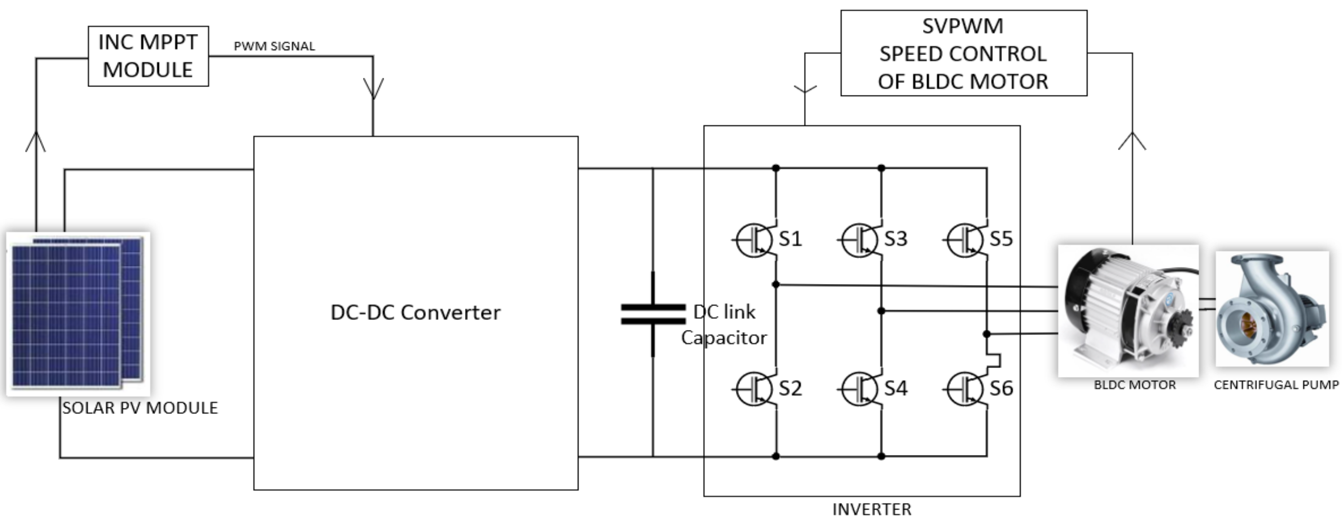

Fig. 1. Block diagram of solar water pumping system.

1.5. OBJECTIVES OF THE PROJECT

The objective of designing the proposed project is to simulate a solar powered water pumping system which offers following features:

a) The system should have high efficiency so that maximum power can be obtained at remote areas as solar every is not completely reliable energy source.
b) The solar pumping system should be easy to understand as technical assistance is not easy in remote areas.
c) Accurate speed control is desirable as system may be used in varying applications that require the pump to operate at different speed.
d) The system should be economic so that maximum number of people can adapt to solar energy and the transition can be profitable as well.

This is achieved by choosing those components which work optimally with each other and achieving control using best possible control techniques.

1.6. OUTLINE OF THE THESIS

The thesis is presented into chapters as follows.

Chapter 2 illustrates designing of SPV array followed by DC-DC converter modelling in Chapter 3. Chapter 4 discusses different controlling techniques used in the system and Chapter 5 constitutes results and discussion followed by conclusion in Chapter 6.

CHAPTER 2: MODELLING OF SPV ARRAY

2.1. INTRODUCTION

Solar photo voltaic energy is a clean source of renewable energy which is contributing in reaching modern country’s energy demands. Many researchers have conducted various research in past decade to improve the methods for modelling and designing of solar cells to move the technology forward. Various models have been developed to evaluate the performance parameters for improvement of the model.

2.2. SPV MODULE SIMULATION THEORY AND DESIGN

Conversion of solar radiation to electrical energy is done by solar cell wafers which are connected electrically to form a solar PV module. Voltage and current value of solar module depends upon the sets of solar cells connected in series and parallel arrays. Solar modules are then wired in series and parallel arrangement and the load requirement dictates the number of panels in array. The representation of a solar cell consists of a diode representing p-n junction and the photoelectric effect is represented by a current source and one resistance in series to simulate Joule effect and one resistance in parallel to compensate for recombination losses. Complete circuit model depicts the function of a solar cell under given radiation condition [15]. For modeling of SPV array, MATLAB Solar panel block is used as it incorporates this model and provides interface to specify key parameters that define an SPV array [16].

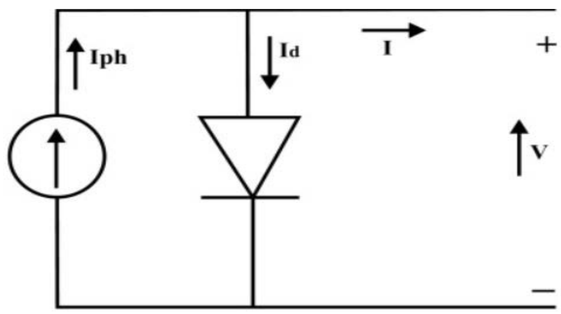

Fig. 2. SPV cell circuit model representation.

SPV array voltage V_{mpp} and current I_{mpp} are maximum power point operating specifications and they are selected to be 136V and 23.55A in designed SPV array. SPV module voltage V_m and current I_m are maximum power point operating specifications and they are selected to be 22.7V and 11.83A in designed SPV module. These values are chosen by the designer. The module open circuit voltage and short circuit current values are also chosen by designer. The open circuit voltage V_{oc} and short circuit current I_{sc} are selected to be 27.2V and 12.92A. Based on these chosen values, number of series and parallel modules is obtained.

Number of solar modules in array wired in series

$$N_s = {}^{V_{mpp}}/_{V_m} = {}^{136}/_{22.7} = 6 \quad (2.1)$$

Number of solar modules in array wired in parallel

$$N_p = {}^{I_{mpp}}/_{I_m} = {}^{23.55}/_{11.83} = 2 \quad (2.2)$$

Power generated by SPV module

$$P_{mpp} = V_{mpp} \times I_{mpp} = 136 \times 23.55 = 3200W \quad (2.3)$$

All these values are given in appendix in tabular form.

2.3. IV AND PV CHARACTERISTICS OF SPV ARRAY

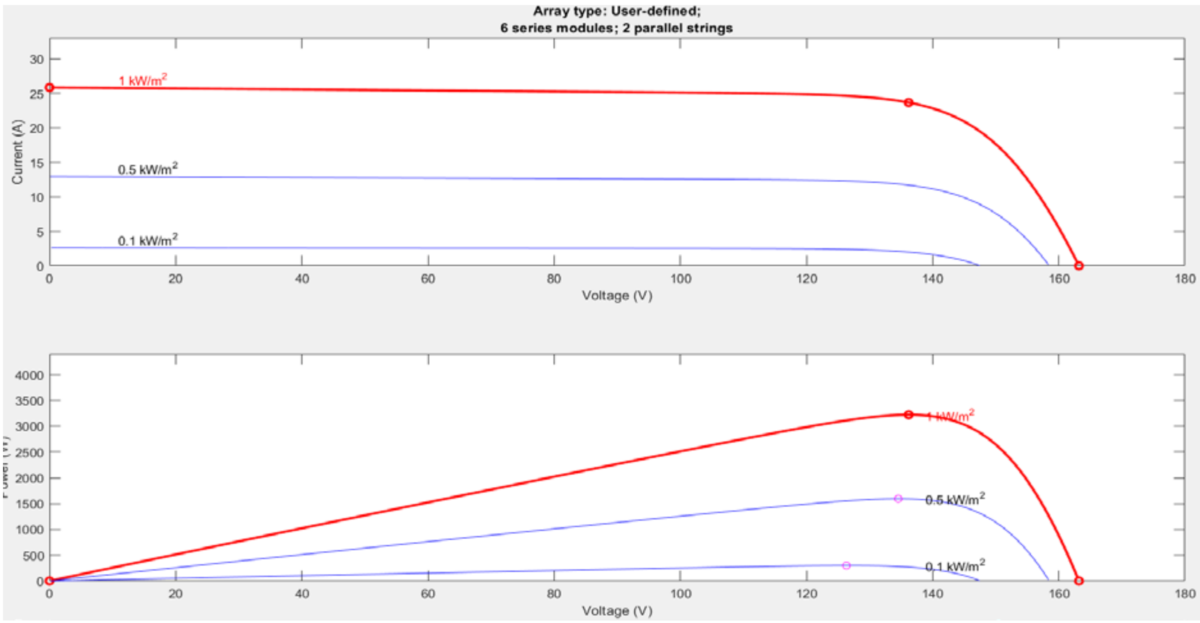

Fig. 3. SPV array IV and PV characteristics.

2.4. CONCLUSION

SPV array modelling is done using MATLAB Simulink successfully as the software facilitates designing of the module by specifying key parameters such as open circuit voltage, maximum power point voltage and current, short circuit current and number of modules to be wired in series array and parallel array to generate required power at a specified load.

CHAPTER 3: DC-DC CONVERTERS

3.1. INTRODUCTION

As the solar insolation level and temperature of surroundings change, the maximum power point of SPV array changes, thus DC-DC converter is necessary. Zeta, Sepic and Cuk converters are very efficient converters and all the three converters are capable of both buck and boost operation. DC-DC converters are essentially a high frequency switching device which is capable of converting one input of one voltage to output of another desired voltage value based on the switching duty ratio of switch.

3.2. ZETA CONVERTER

3.2.1. SCHEMATIC DIAGRAM AND THEORY

Zeta converter is evolved from buck boost converter design. Buck boost converter output is inverted while in Zeta converter, positive polarity output is obtained. Fig. 4 shows circuit diagram of Zeta converter. Voltage gains and higher efficiency is there in Zeta converter compared to buck boost converter [17].

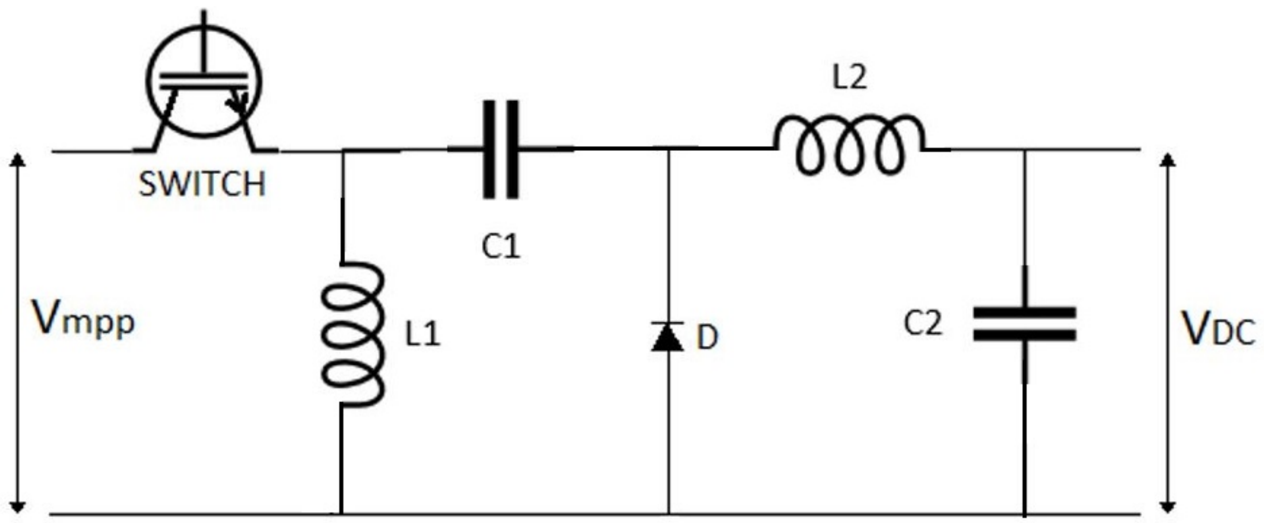

Fig. 4. Zeta converter schematic circuit diagram.

3.2.2. DESIGN OF ZETA CONVERTER

Zeta converter is a DC-DC converter which is employed in this project to utilize maximum power of SPV array by operating at point of maximum power regardless of solar insolation level and ambient temperature. The solar panel maximum voltage is 136V at peak insolation of 1000W/m^2. The switching frequency for Zeta converter is chosen to be 30KHz. The MPPT module uses INC algorithm to calculate duty cycle for Zeta converter to extract maximum power. Zeta converter evolved from buck boost converter but output of Zeta converter is of positive polarity contrary to buck boost converter. Calculations for all the components is done taking ripple of 10%. The selection of values for the components used in Zeta converter depends on output side BLDC motor parameters and input side SPV array parameters shown in appendix.

Zeta converter calculations are given below.

$$\text{Duty ratio} = \frac{V_{dc}}{V_{dc}+V_{mpp}} = \frac{200}{200+136} = 0.595 \quad (3.1)$$

$$L_1 = \frac{D.V_{mpp}}{f_s.\Delta I_{L1}} = \frac{0.595*136}{30000*(23.55*0.1)} = 1.9\ \text{mH} \quad (3.2)$$

$$L_2 = \frac{(1-D).V_{dc}}{f_s.\Delta I_{L2}} = \frac{(1-0.595)*200}{30000*(16*0.1)} = 2.81\ \text{mH} \quad (3.3)$$

$$C_1 = \frac{D.I_{dc}}{f_s.\Delta V_{C1}} = \frac{0.595*16}{30000*(200*0.1)} = 15.8\ \mu\text{F} \quad (3.4)$$

The Zeta converter output is conditioned using a DC link capacitor C_2. DC link capacitor rated and minimum values C_{2rated} and C_{2min} are calculated for ω_r and ω_{min} which is the rated and minimum angular speed of BLDC motor as shown below.

$$\omega_r = \frac{2\pi N_r.P}{120} = \frac{2\pi*3000*6}{120} = 942\text{rad/s} \quad (3.5)$$

$$\omega_{min} = \frac{2\pi N_{min}.P}{120} = \frac{2\pi*1500*6}{120} = 471\text{rad/s} \quad (3.6)$$

$$C_{2rated} = \frac{I_{dc}}{6.\omega_{rated}.\Delta V_{dc}} = \frac{16}{6*941*(200*0.1)} = 141.69\mu F \quad (3.7)$$

$$C_{2min} = \frac{I_{dc}}{6.\omega_{min}.\Delta V_{dc}} = \frac{16}{6*471*(200*0.1)} = 283.08\mu F \quad (3.8)$$

DC link capacitor C_2 value is selected 283.08μF as C_{2min}.

3.2.3. SIMULATION BLOCK DIAGRAM

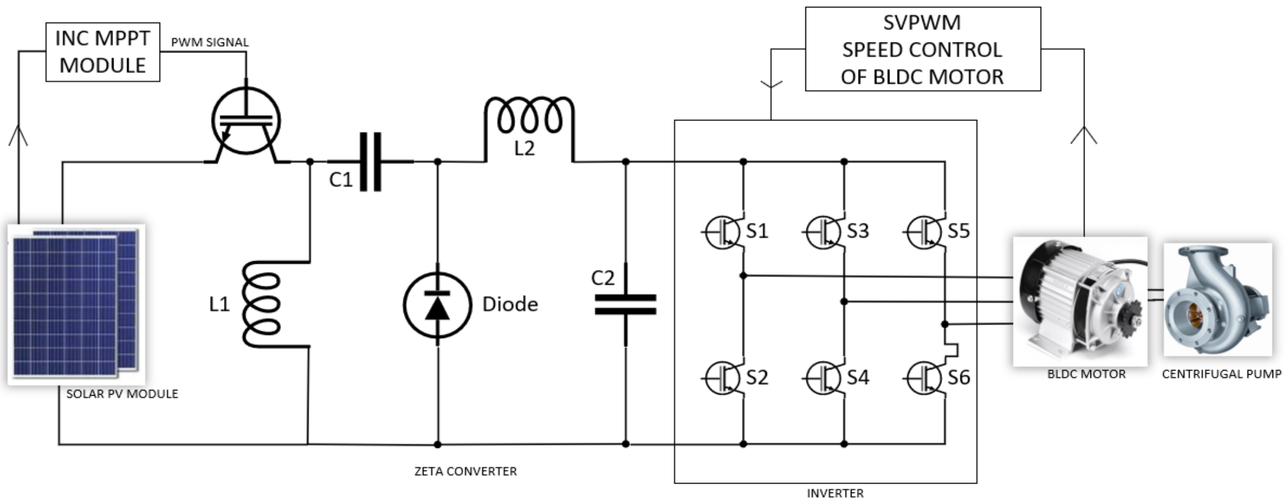

Fig. 5. Simulation block diagram utilizing Zeta converter.

3.3. SEPIC CONVERTER

3.3.1. SCHEMATIC DIAGRAM AND THEORY

Sepic converter evolved from boost converter and it can be derived as a buck and boost converter in cascade design. In Sepic converter, positive polarity output is obtained similar to Zeta converter [18]. Sepic converter circuit is shown in Fig. 6.

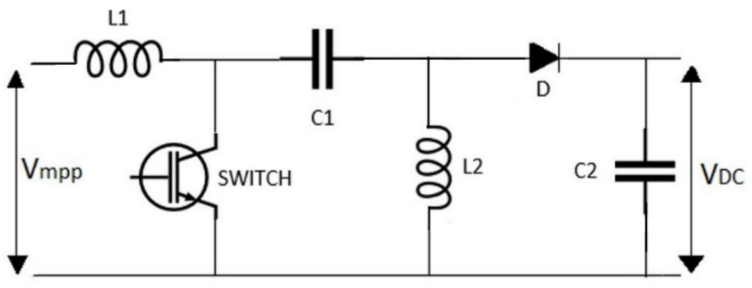

Fig. 6. Sepic converter schematic circuit diagram.

3.3.2. DESIGN OF SEPIC CONVERTER

Sepic converter is a DC-DC converter which is employed in this project to utilize maximum power of SPV array by maintaining the operating point at point of maximum power regardless of solar insolation level and ambient temperature variation. The solar panel maximum voltage is 136V at peak insolation of $1000W/m^2$. The switching frequency for Sepic converter is chosen to be 30KHz. The MPPT module uses INC algorithm to calculate duty cycle for Sepic converter to extricate maximum power. Sepic converter evolved from boost converter and it can be derived as a buck and boost converter in cascade design. Calculations for all the components is done taking ripple of 10%. The selection of values for the components used in Sepic converter depends on output side BLDC motor parameters and input side SPV array parameters shown in appendix.

Sepic converter calculations are given below.

$$\text{Duty ratio} = \frac{V_{dc}}{V_{dc}+V_{mpp}} = \frac{200}{200+136} = 0.595 \tag{3.9}$$

$$L_1 = \frac{D.V_{mpp}}{f_s.\Delta I_{L1}} = \frac{0.595*136}{30000*(23.55*0.1)} = 1.9\text{ mH} \tag{3.10}$$

$$L_2 = \frac{(1-D).V_{dc}}{f_s.\Delta I_{L2}} = \frac{(1-0.595)*200}{30000*(16*0.1)} = 2.81\text{ mH} \tag{3.11}$$

$$C_1 = \frac{D.I_{dc}}{f_s.\Delta V_{C1}} = \frac{0.595*16}{30000*(200*0.1)} = 15.8\ \mu F \tag{3.12}$$

The Sepic converter output is conditioned using a DC link capacitor C_2. DC link capacitor rated and minimum values C_{2rated} and C_{2min} are calculated for ω_r and ω_{min} which is the rated and minimum angular speed of BLDC motor as shown below.

$$\omega_r = \frac{2\pi N_r.P}{120} = \frac{2\pi*3000*6}{120} = 942\text{rad/s} \tag{3.13}$$

$$\omega_{min} = \frac{2\pi N_{min}.P}{120} = \frac{2\pi*1500*6}{120} = 471\text{rad/s} \tag{3.14}$$

$$C_{2rated} = \frac{I_{dc}}{6.\omega_{rated}.\Delta V_{dc}} = \frac{16}{6*941*(200*0.1)} = 141.69\mu F \tag{3.15}$$

$$C_{2min} = \frac{I_{dc}}{6.\omega_{min}.\Delta V_{dc}} = \frac{16}{6*471*(200*0.1)} = 283.08\mu F \tag{3.16}$$

DC link capacitor C_2 value is selected 283.08μF as C_{2min}.

3.3.3. SIMULATION BLOCK DIAGRAM

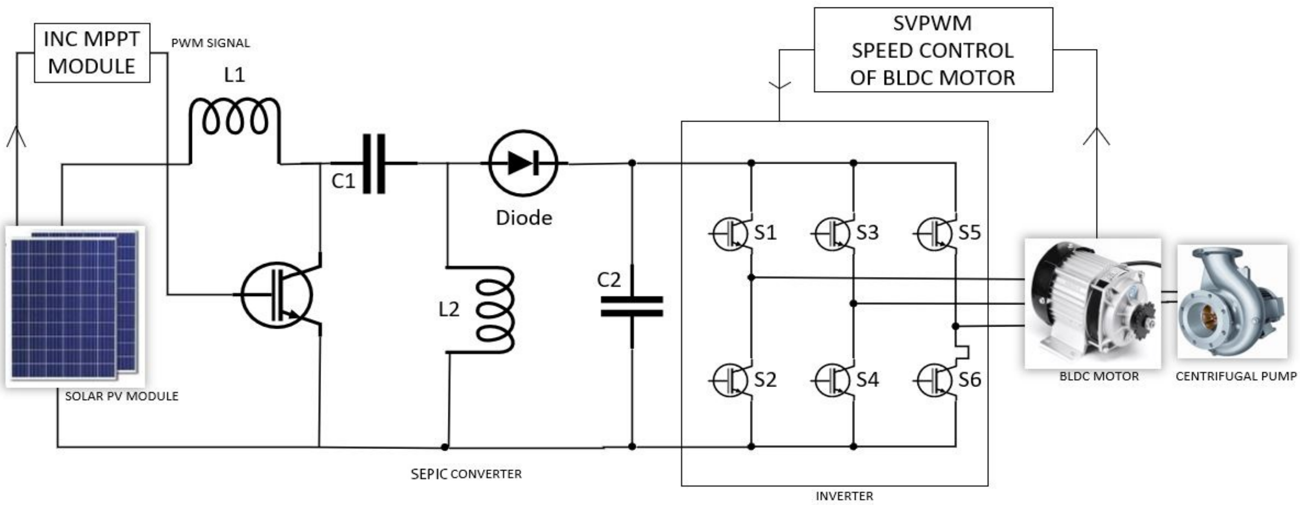

Fig. 7. Simulation block diagram utilizing Sepic converter.

3.4. CUK CONVERTER

3.4.1. SCHEMATIC DIAGRAM AND THEORY

Cuk converter is evolved from boost converter design and it can be realized as a boost and buck converter in cascade design. In Cuk converter, inverted polarity output is obtained similar to buck-boost converter [19]. Cuk converter circuit diagram is shown in Fig. 8.

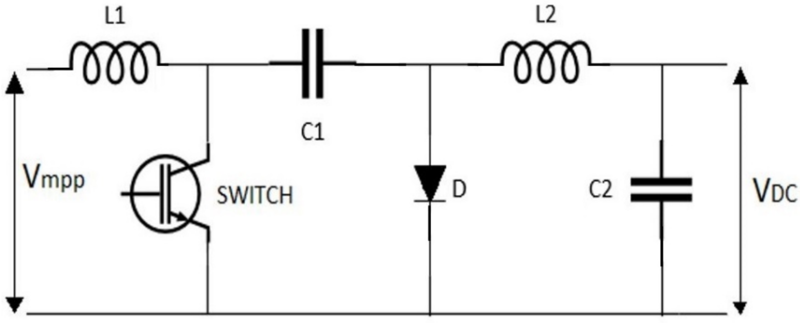

Fig. 8. Cuk converter schematic circuit diagram.

3.4.2. DESIGN OF CUK CONVERTER

Cuk converter is employed in this project to utilize maximum power of SPV array by operating at point of maximum power regardless of ambient temperature and solar insolation level. The solar panel maximum voltage is 136V at peak insolation of 1000W/m^2. The switching frequency for Cuk converter is chosen to be 30KHz. The MPPT module uses INC algorithm to calculate duty cycle for Cuk converter to extract maximum power. Cuk converter is evolved from boost converter design and it can be realized as a boost and buck converter in cascade design. Cuk converter output is inverted with respect to reference. Calculations for all the components is done taking ripple of 10%. The selection of values for the components used in Cuk converter depends on output side BLDC motor parameters and input side SPV array parameters shown in appendix.

Cuk converter calculations are given below.

$$\text{Duty ratio} = \frac{V_{dc}}{V_{dc}+V_{mpp}} = \frac{200}{200+136} = 0.595 \quad (3.17)$$

$$L_1 = \frac{D.V_{mpp}}{f_s.\Delta I_{L1}} = \frac{0.595*136}{30000*(23.55*0.1)} = 1.9\ \text{mH} \quad (3.18)$$

$$L_2 = \frac{D.V_{mpp}}{f_s.\Delta I_{L2}} = \frac{0.595*136}{30000*(16*0.1)} = 1.68\ \text{mH} \quad (3.19)$$

$$C_1 = \frac{(1-D).I_{mpp}}{f_s.\Delta V_{C1}} = \frac{(1-0.595)*23.55}{30000*(200*0.1)} = 0.95\ \mu\text{F} \quad (3.20)$$

The Cuk converter output is conditioned using a DC link capacitor C_2. DC link capacitor rated and minimum values C_{2rated} and C_{2min} are calculated for ω_r and ω_{min} which is the rated and minimum angular speed of BLDC motor as shown below.

$$\omega_r = \frac{2\pi N_r.P}{120} = \frac{2\pi*3000*6}{120} = 942\text{rad/s} \quad (3.21)$$

$$\omega_{min} = \frac{2\pi N_{min}.P}{120} = \frac{2\pi*1500*6}{120} = 471\text{rad/s} \quad (3.22)$$

$$C_{2rated} = \frac{I_{dc}}{6.\omega_{rated}.\Delta V_{dc}} = \frac{16}{6*941*(200*0.1)} = 141.69\mu F \tag{3.23}$$

$$C_{2min} = \frac{I_{dc}}{6.\omega_{min}.\Delta V_{dc}} = \frac{16}{6*471*(200*0.1)} = 283.08\mu F \tag{3.24}$$

DC link capacitor C_2 value is selected 283.08μF as C_{2min}.

3.4.3. SIMULATION BLOCK DIAGRAM

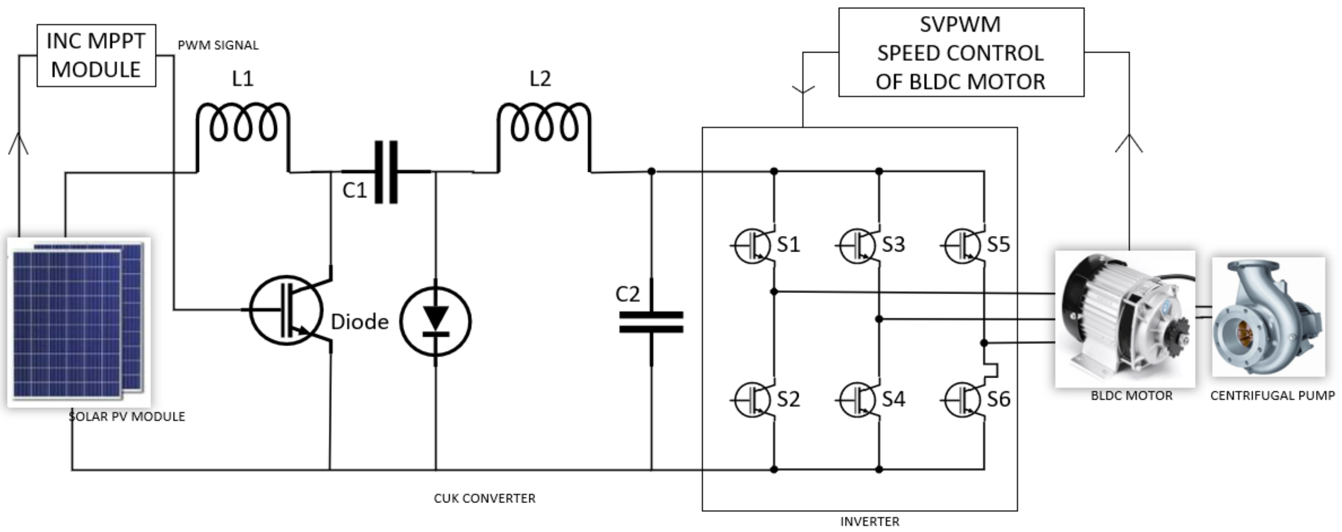

Fig. 9. Simulation block diagram utilizing Cuk converter.

3.5. CONCLUSION

Zeta, Sepic and Cuk converters are successfully modelled in MATLAB Simulink environment and simulated along complete simulation successfully. Controlling techniques and specification of BLDC motor are discussed in further chapters.

CHAPTER 4: CONTROL TECHNIQUES

4.1. INTRODUCTION

Solar water pumping system is a complex system which requires controlling mechanism at different stages in order to achieve desired parameters such as BLDC motor speed and DC-DC converter output voltage. The BLDC motor speed, shaft angle of motor is measured and taken as feedback to control speed using SVPWM speed control. DC-DC converter output voltage is controlled by measuring converter input voltage and current and using INC algorithm to maintain point of maximum power. These techniques are discussed in further section.

4.2. MAXIMUM POWER POINT TRACKING (MPPT)

4.2.1. MPPT THEORY

MPPT is a widely used technique which helps in utilization of maximum amount of usable or available power from SPV array. Various MPPT techniques have been developed over the years to improve the efficiency of solar powered setups. MPPT technique works by measuring voltage and current output at terminals of SPV array at a very fast rate and then runs algorithm to find the best duty ratio for a DC-DC converter which facilitates the utilization of maximum power.

INC algorithm has been used in this project as MPPT technique and it controls Zeta, Sepic and Cuk converter and comparison is made. INC algorithm calculates duty ratio adjustment in real time to find a duty ratio which satisfies the condition $\frac{dI_{PV}}{dV_{PV}} + \frac{I_{PV}}{V_{PV}} = 0$. The condition for optimal duty ratio according to INC algorithm is that when instantaneous conductance and incremental conductance add up to zero and that duty ratio corresponds to the maximum power point [21]. $\frac{I_{PV}}{V_{PV}}$ represents instantaneous and $\frac{dI_{PV}}{dV_{PV}}$ represents incremental conductance. INC algorithm flow graph and program code are shown in further sections [22].

4.2.2. INC MPPT FLOW GRAPH

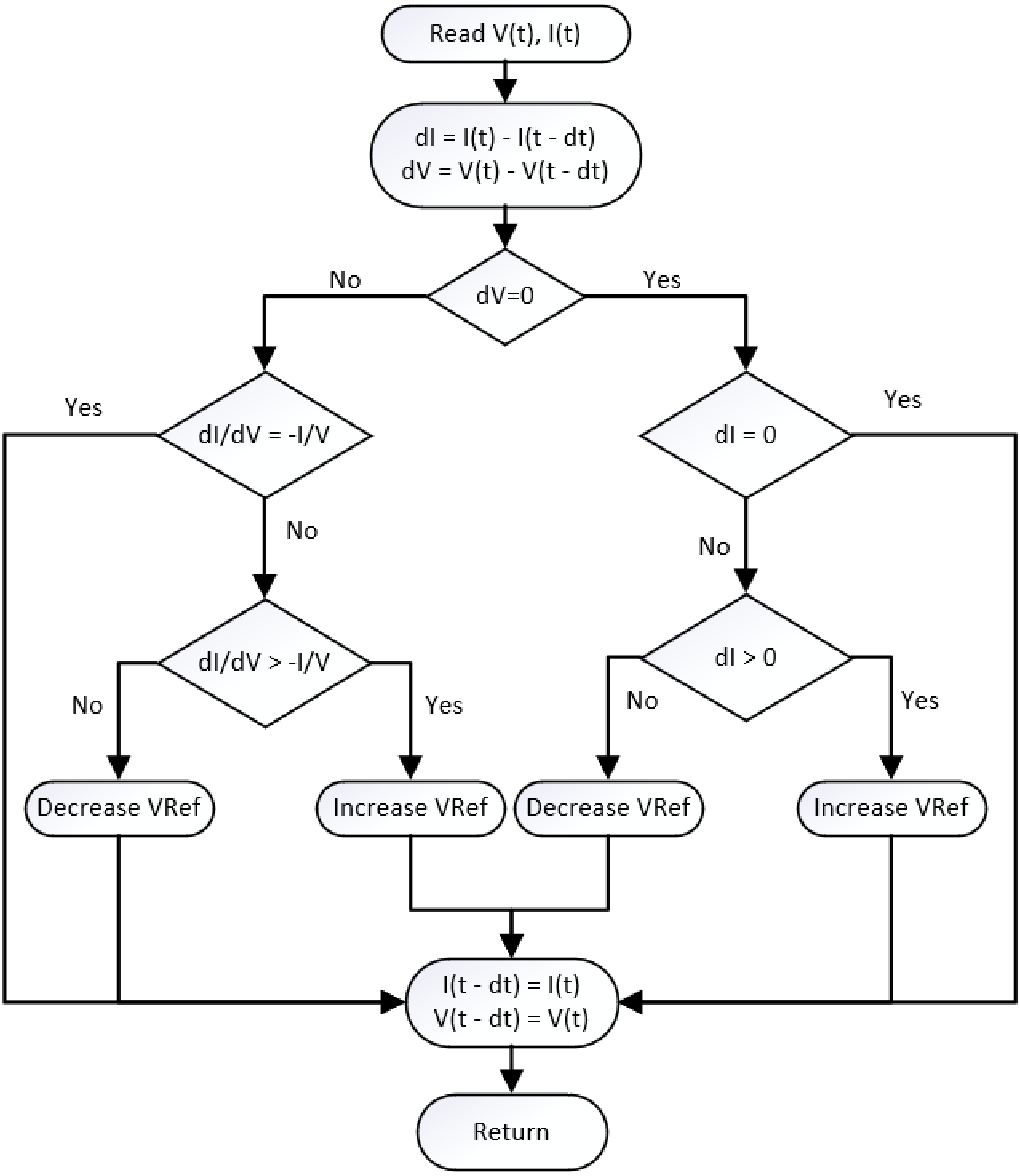

Fig. 10. INC MPPT algorithm flow graph.

4.2.3. INC MPPT PROGRAM CODE

```
function Dutyratio = INC(Vpv,Ipv)  //start of code
Delta = 0.0001;
dutyratio_initial = 0.52;
dutyratio_minimum = 0.83;
dutyratio_maximum = 0.32;

persistent Vold dutyratio_old Iold;

if empty(Vold)
   Vold=0;
   Iold=0;
   dutyratio_old=dutyratio_init;
end
delV = Vpv - Vold;
delI = Ipv - Iold;

if delV == 0
   if delI == 0
      Dutyratio = dutyratio_old;
   else
      if delI > 0
         Dutyratio=dutyratio_old - Delta;
      else
         Dutyratio=dutyratio_old + Delta;
      end
   end

else
   if delI/delV == -Ipv/Vpv
      Dutyratio = dutyratio_old;
   else
      if delI/delV > -Ipv/Vpv
         Dutyratio=dutyratio_old - Delta;
      else
         Dutyratio=dutyratio_old + Delta;
      end
   end
end

if Dutyratio >= dutyratio_max || Dutyratio <= dutyratio_min
   Dutyratio = dutyratio_old;
end
dutyratio_old=Dutyratio;
Vold=Vpv;
Iold=Ipv;  //end of code
```

4.3. SPEED CONTROL OF BLDC MOTOR

4.3.1. SVPWM SPEED CONTROL THEORY

The speed control of BLDC motor is attained using SVPWM technique along with six-pulse inverter. This technique is capable of providing varying voltage and frequency output for BLDC motor. SVPWM is a field-oriented control where voltage reference vector is generated using feedback from BLDC motor output. The angle and magnitude of the vector is adjusted at a very high frequency to achieve desired magnetic field vector position. BLDC motor rotor angle is taken as feedback after clarke and park transform and 3 PI controllers are used to minimize error by generating direct axis and quadrature axis reference voltage vectors. The six fundamental vector directions are shown in Fig. 11 [23]. High speed switching is done between any two vectors and center position to produce field vector of desired magnitude and direction [24]. This method proves to be better than sinusoidal PWM due to ease of digital realization and better use of DC link voltage which translated to higher efficiency of operation [25].

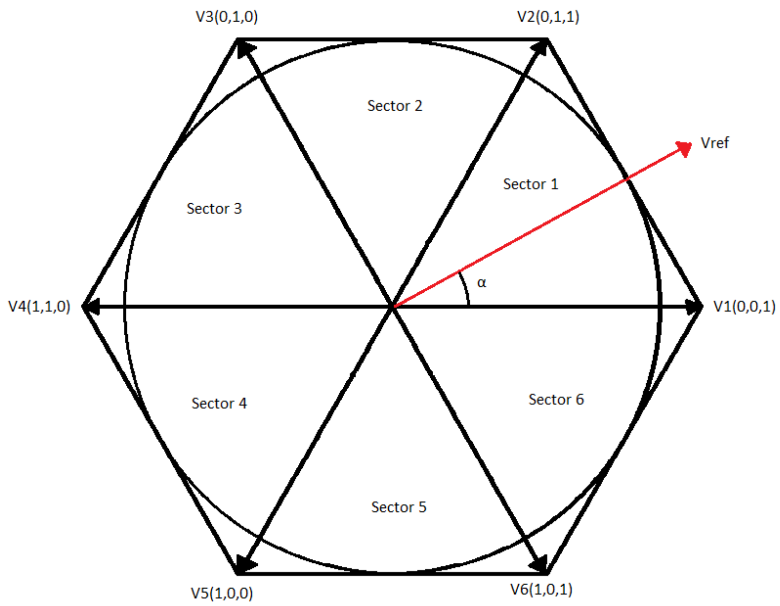

Fig. 11. Space vector diagram and reference representation.

4.3.2. SVPWM SPEED CONTROL BLOCK DIAGRAM

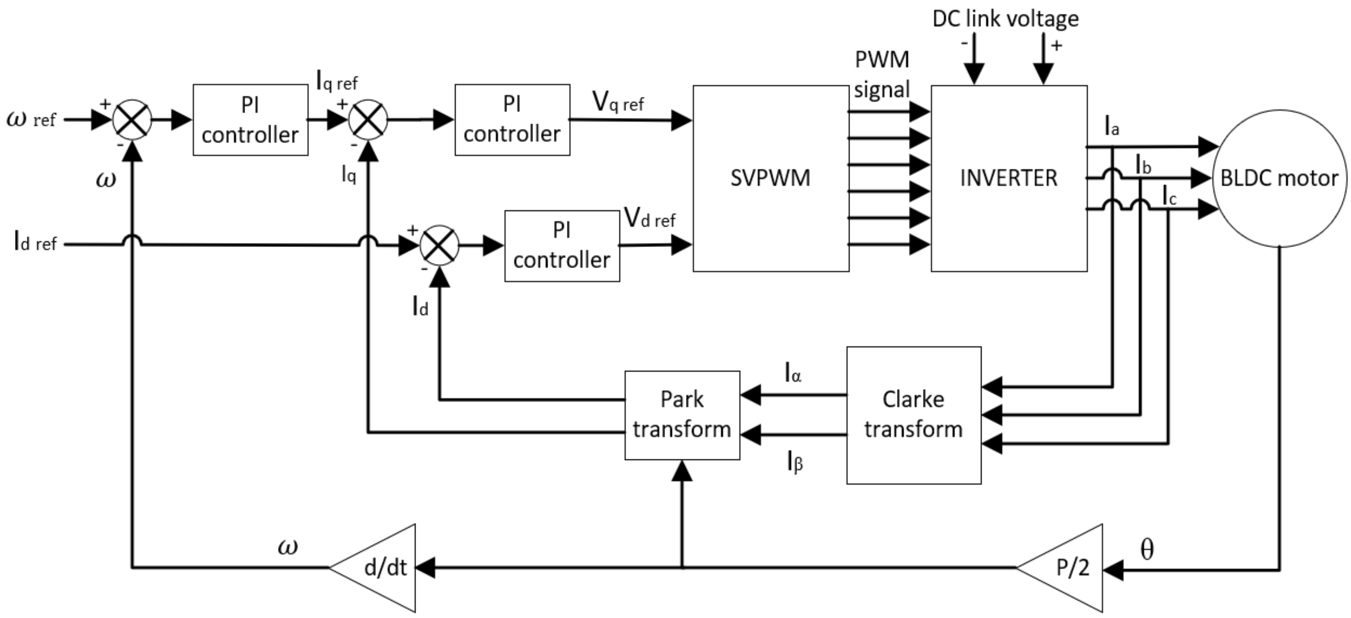

Fig. 12. SVPWM speed control block diagram.

4.3.3. SVPWM TECHNIQUE BLOCK DIAGRAM

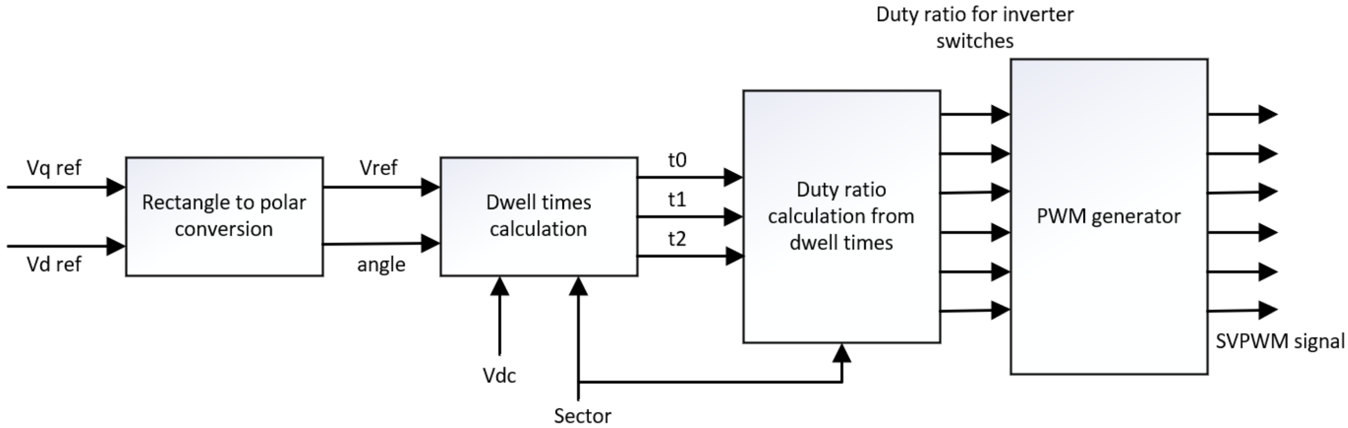

Fig. 13. SVPWM technique block diagram which is a sub block in SPVWM speed control schematic block diagram.

4.4. CONCLUSION

INC MPPT module and SVPWM speed control are successfully simulated and used with complete simulation at specific stages to control specific parameters.

CHAPTER 5: RESULTS & DISCUSSION

5.1. SPV ARRAY AND BLDC MOTOR RESULTS

5.1.1. STEADY STATE OUTPUT AT PEAK INSOLATION

The SPV array characteristics are shown in Fig. 14. The insolation level is set at 1000W/m^2 the SPV output is plotted. It is evident from the characteristics that the maximum power is being extracted at 136V from solar panels rated at 3.2kW.

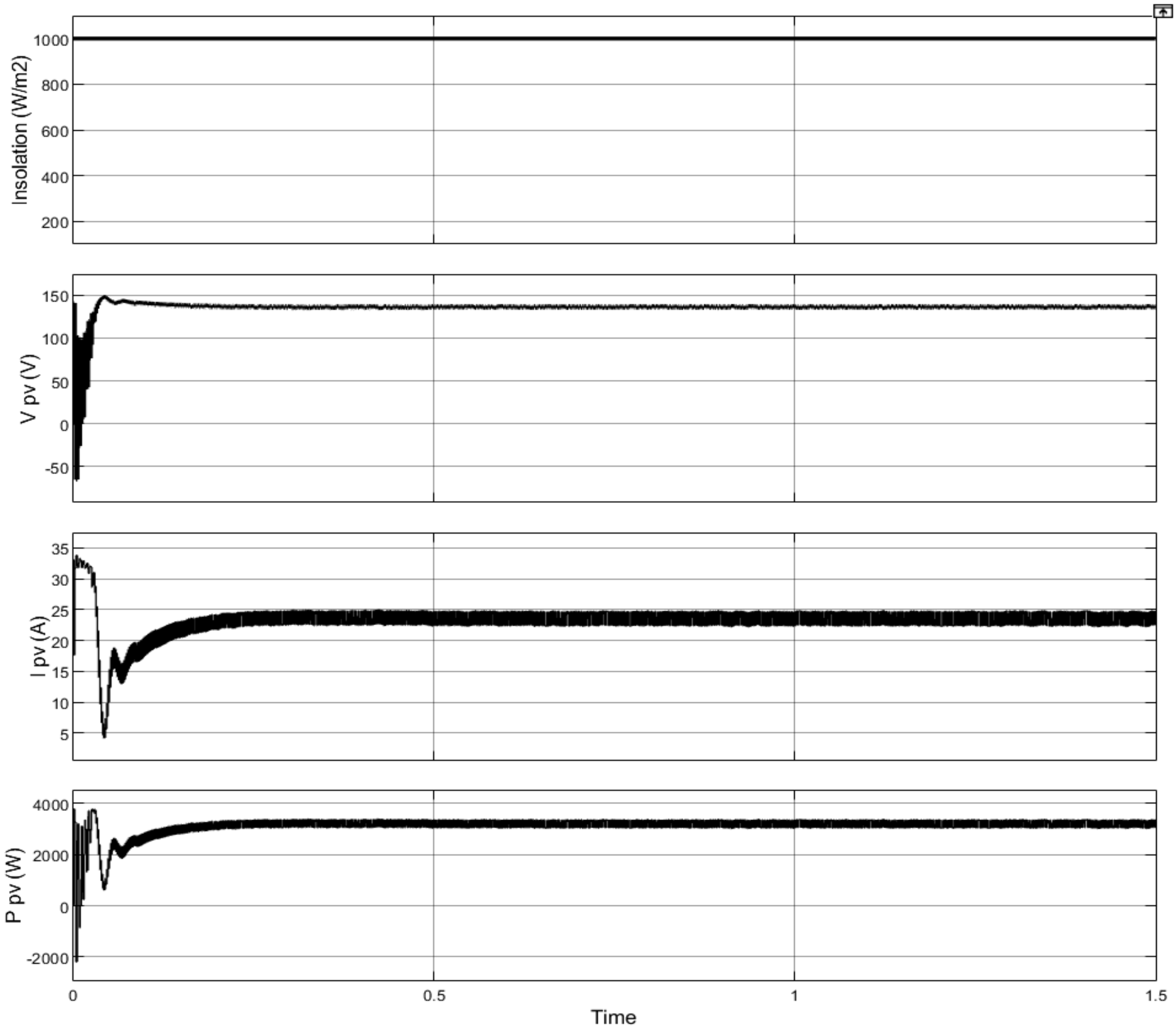

Fig. 14. SPV array peak insolation output at 1000W/m^2.

The BLDC motor characteristics are shown in Fig. 15. The converter is able to maintain 200V DC link voltage without any ripples and BLDC motor is operating at 3000RPM of rated speed without any ripples. Motor output torque is also maintained at 9.1Nm with 2Nm peak to peak ripples which are to be expected in a BLDC motor. As all the converters are able to sustain DC link voltage of 200V at rated load, performance characteristics of BLDC motor and SPV array remain unchanged at steady state.

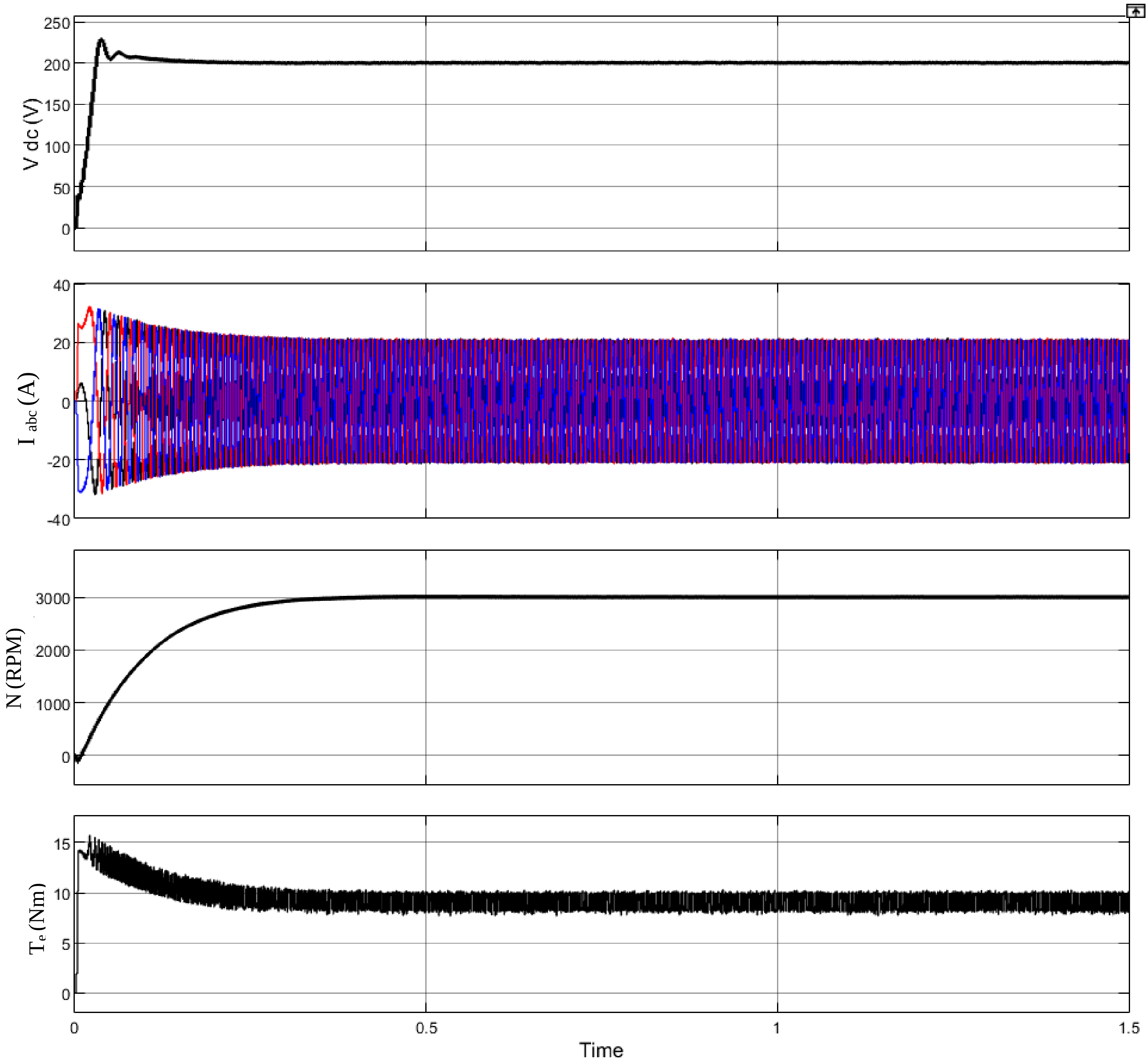

Fig. 15. BLDC motor peak insolation output at 1000W/m^2.

5.1.2. OUTPUT AT VARYING INSOLATION LEVEL

The simulation is tested starting from peak solar insolation level of 1000 W/m^2 for steady state analysis of the DC-DC converters. The insolation level is then decreased to 200W/m^2 in order to examine the transient behavior after which the insolation level is taken to 900W/m^2 to test performance of system below peak insolation. The Solar insolation characteristics and SPV array output characteristics are shown in Fig. 16.

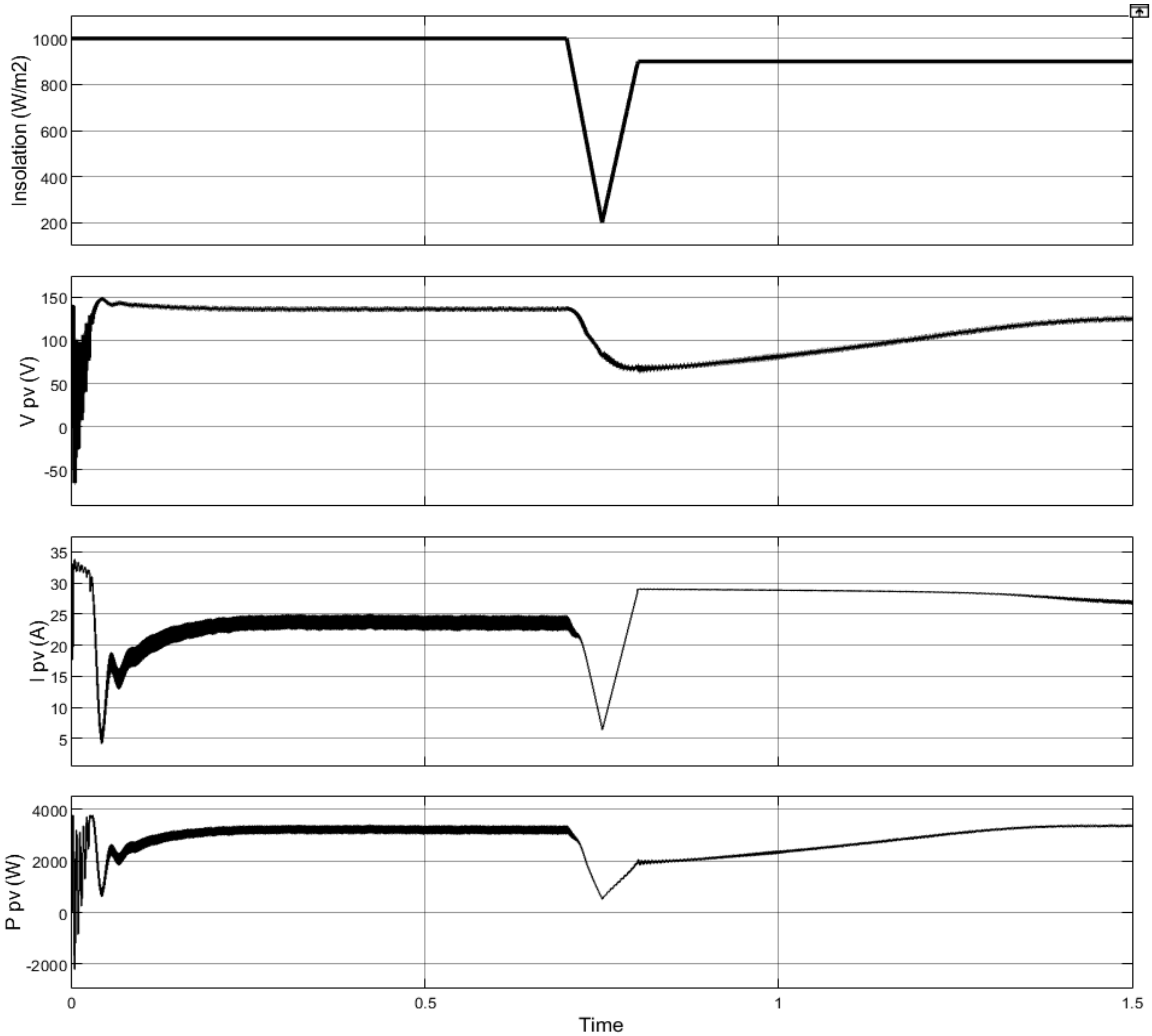

Fig. 16. SPV array output characteristics for varying insolation.

SPV array voltage and current variation can be observed for change in insolation level to ensure maximum power extraction. BLDC motor output characteristics during solar insolation variation is given in Fig. 17. The BLDC motor characteristics indicate successful recovery of motor speed to 3000RPM but motor torque drops to 8.9Nm and torque ripple has increased to 2.6Nm peak to peak during insolation level recovery to 900W/m^2.

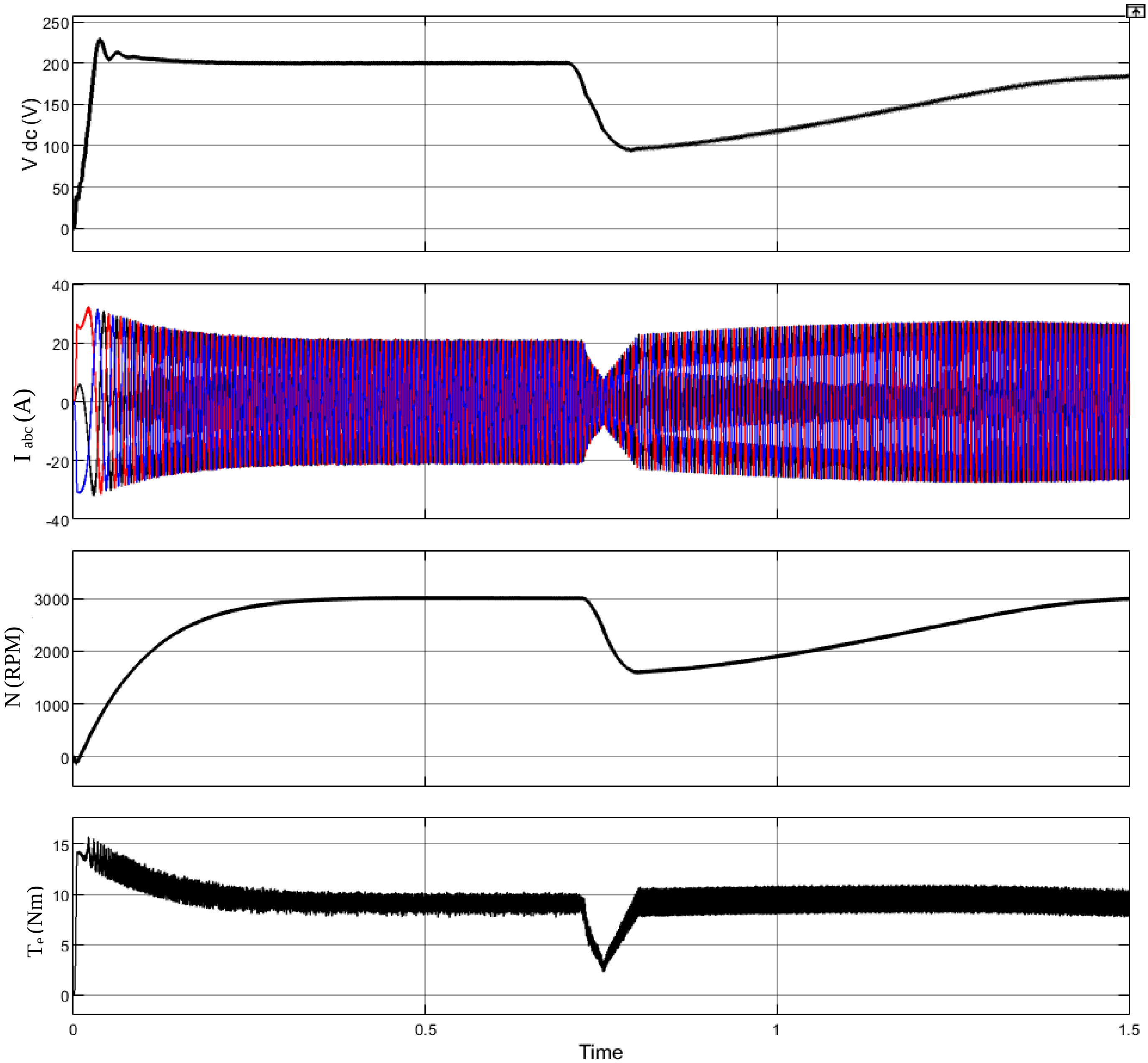

Fig. 17. BLDC motor output characteristics for varying insolation.

5.2. ZETA CONVERTER INTERNAL CHARACTERISTICS

5.2.1. STEADY STATE OUTPUT AT PEAK INSOLATION

Zeta converter characteristics as shown in Fig. 18 show ripples under 10% during peak steady insolation level of 1000W/m^2 which is under specified tolerance limit. Peak insolation characteristics are similar compared to Sepic and Cuk converter except capacitor voltage stress which is 200V which is in-between Sepic and Cuk converter.

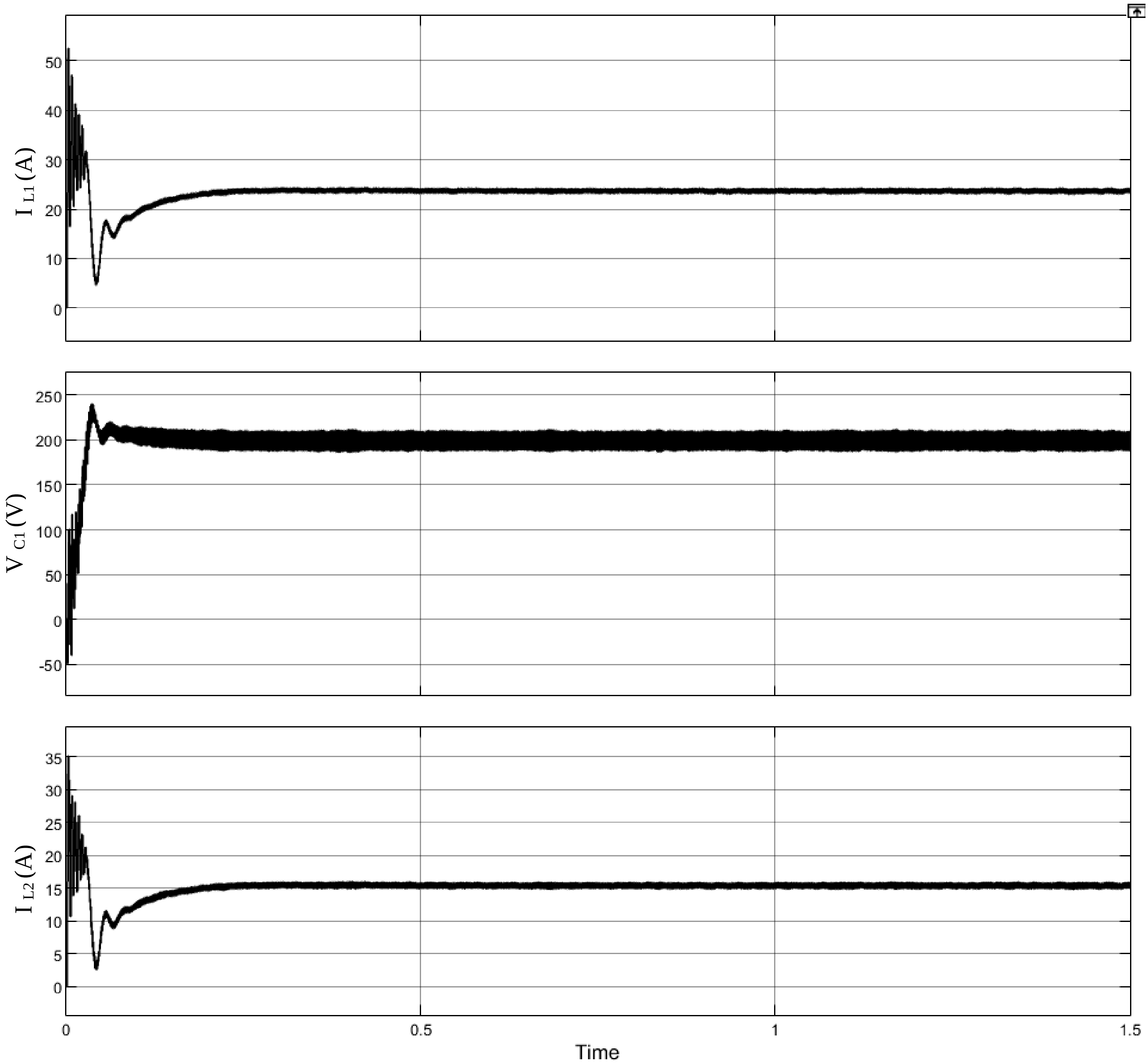

Fig. 18. Zeta converter characteristics for peak insolation of 1000W/m^2.

5.2.2. OUTPUT AT VARYING INSOLATION LEVEL

Zeta converter is subjected to steady state, drooping and recovering insolation levels as shown in Fig. 16. After insolation drop and recovery to 900W/m^2, converter parameters successfully recover to steady values as shown in Fig. 19. Zeta converter input and output inductor current and capacitor voltage show maximum ripples amongst three converters that last for 0.1s before recovering to steady state values.

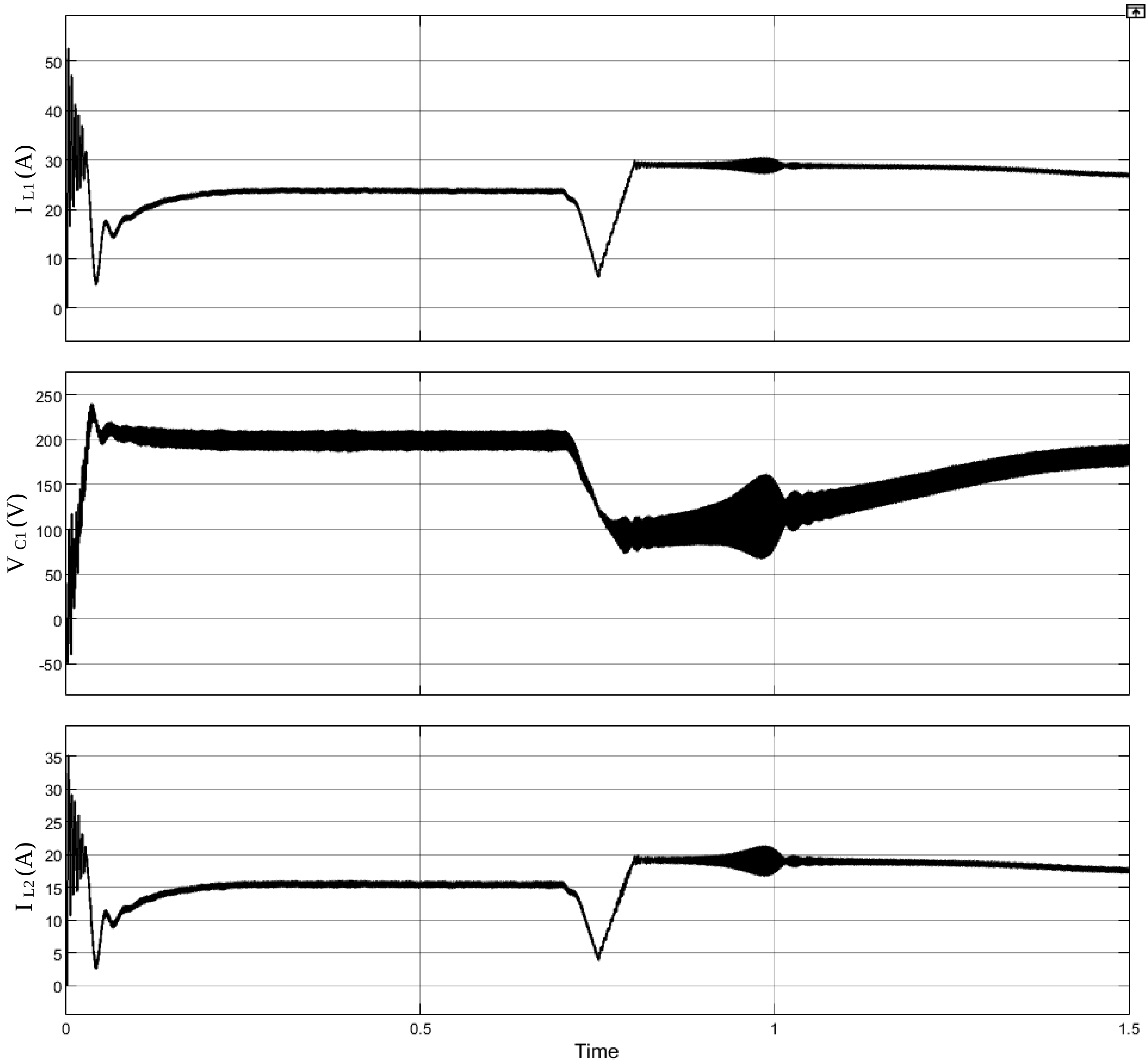

Fig. 19. Zeta converter characteristics for varying insolation level.

5.3. SEPIC CONVERTER INTERNAL CHARACTERISTICS

5.3.1. STEADY STATE OUTPUT AT PEAK INSOLATION

Sepic converter characteristics as shown in Fig. 20 show ripples under 10% during peak steady insolation level of 1000W/m^2 which is under specified tolerance limit. Peak insolation characteristics are similar compared to Zeta and Cuk converter except capacitor voltage stress which is 140V which is less compared to Zeta and Cuk converter.

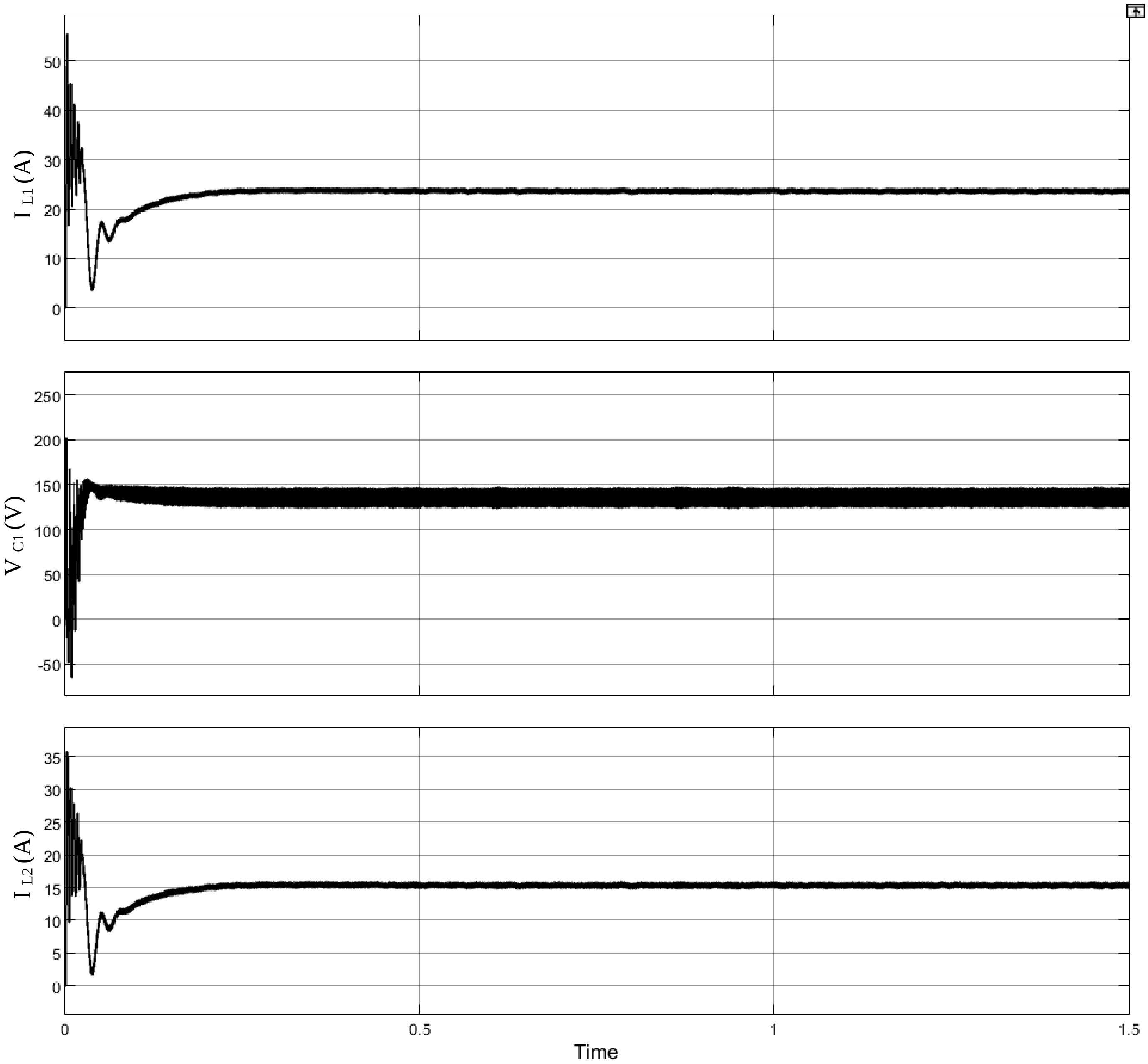

Fig. 20. Sepic converter characteristics for peak insolation of 1000W/m^2.

5.3.2. OUTPUT AT VARYING INSOLATION LEVEL

Sepic converter is subjected to steady state, drooping and recovering insolation levels as shown in Fig. 16. After insolation drop and recovery to 900W/m^2, converter parameters successfully recover to steady values as shown in Fig. 21. Sepic converter input and output inductor current and capacitor voltage show no ripples.

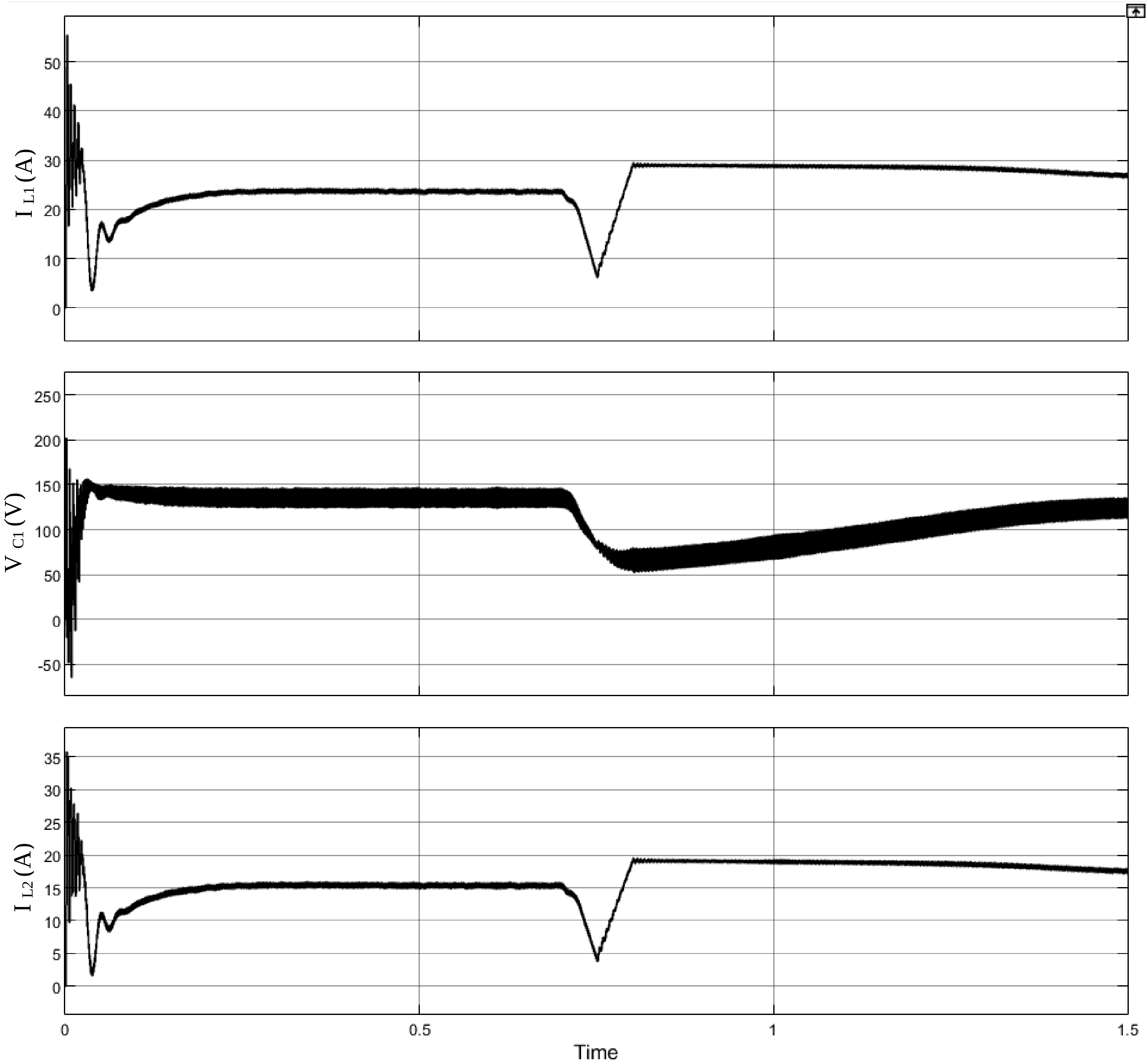

Fig. 21. Sepic converter characteristics for varying insolation level.

5.4. CUK CONVERTER INTERNAL CHARACTERISTICS

5.4.1. STEADY STATE OUTPUT AT PEAK INSOLATION

Cuk converter characteristics as shown in Fig. 22 show ripples under 10% during peak steady insolation level of 1000W/m^2 which is under specified tolerance limit. Peak insolation characteristics are similar compared to Zeta and Cuk converter except capacitor voltage stress which is 340V which is less compared to Zeta and Cuk converter.

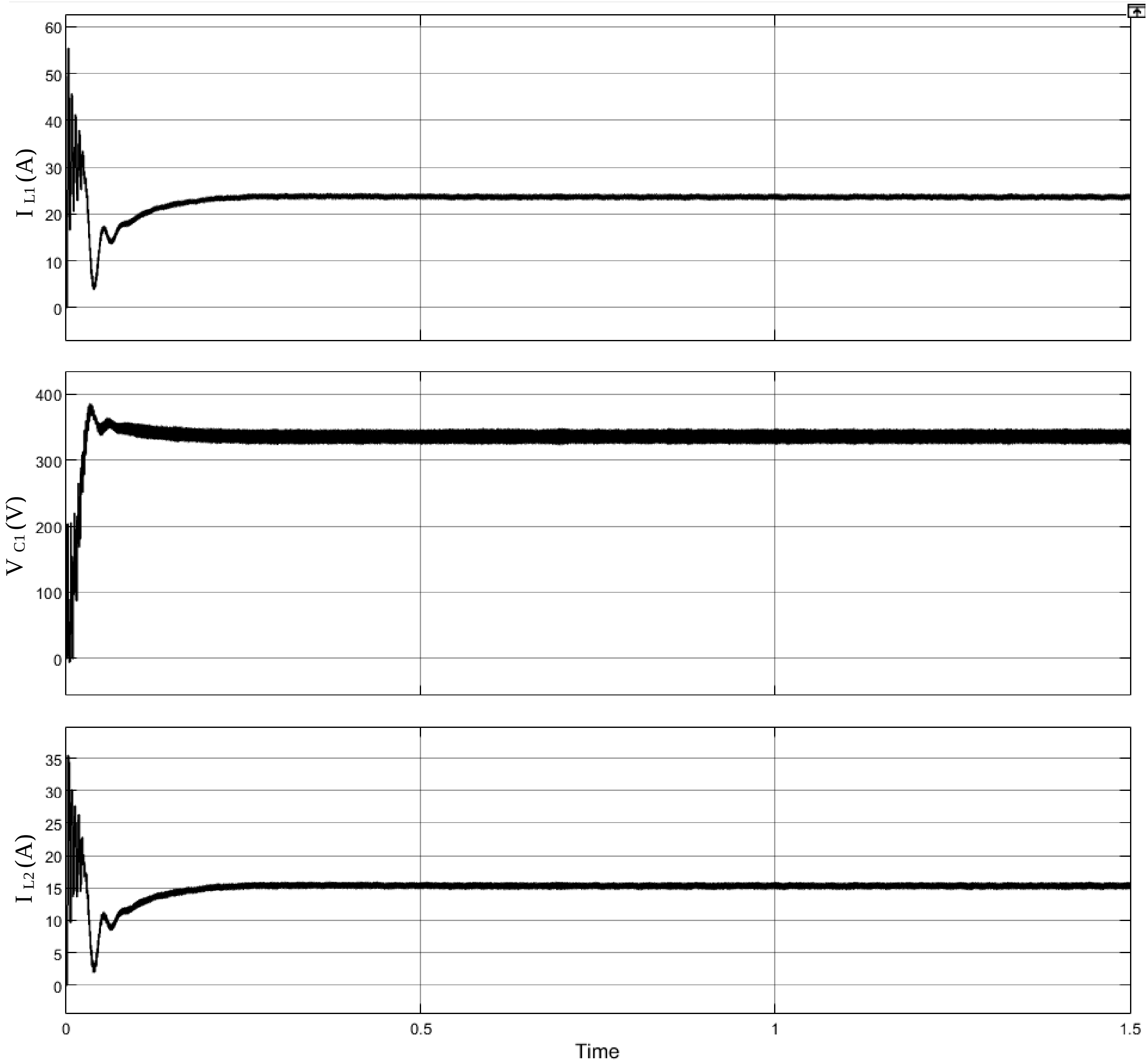

Fig. 22. Cuk converter characteristics for peak insolation of 1000W/m^2.

5.4.2. OUTPUT AT VARYING INSOLATION LEVEL

Cuk converter is subjected to steady state, drooping and recovering insolation levels as shown in Fig. 16. After insolation drop and recovery to 900W/m^2, converter parameters successfully recover to steady values as shown in Fig. 23. Cuk converter input and output inductor current and capacitor voltage show ripples which are less compared to Zeta converter.

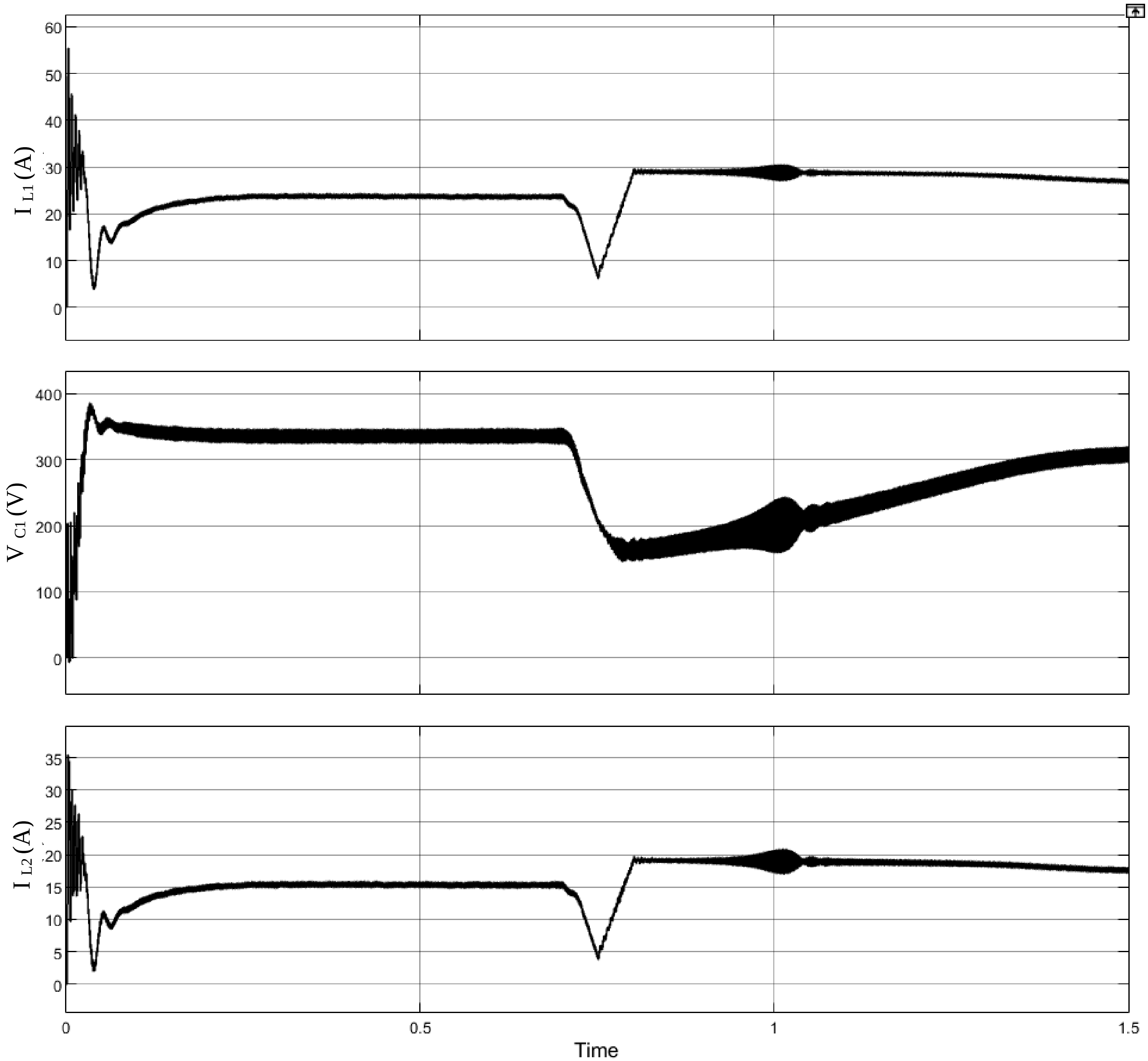

Fig. 23. Cuk converter characteristics for varying insolation level.

5.5. DC LINK VOLTAGE BUILD UP CHARACTERISTICS FOR ZETA, SEPIC AND CUK CONVERTERS

The DC link voltage build up during starting for all the three converters is shown in Fig. 24. Transient behavior during starting is different for Zeta, Sepic and Cuk converter. Sepic converter shows the least rise time and peak time followed by Cuk and Zeta converter.

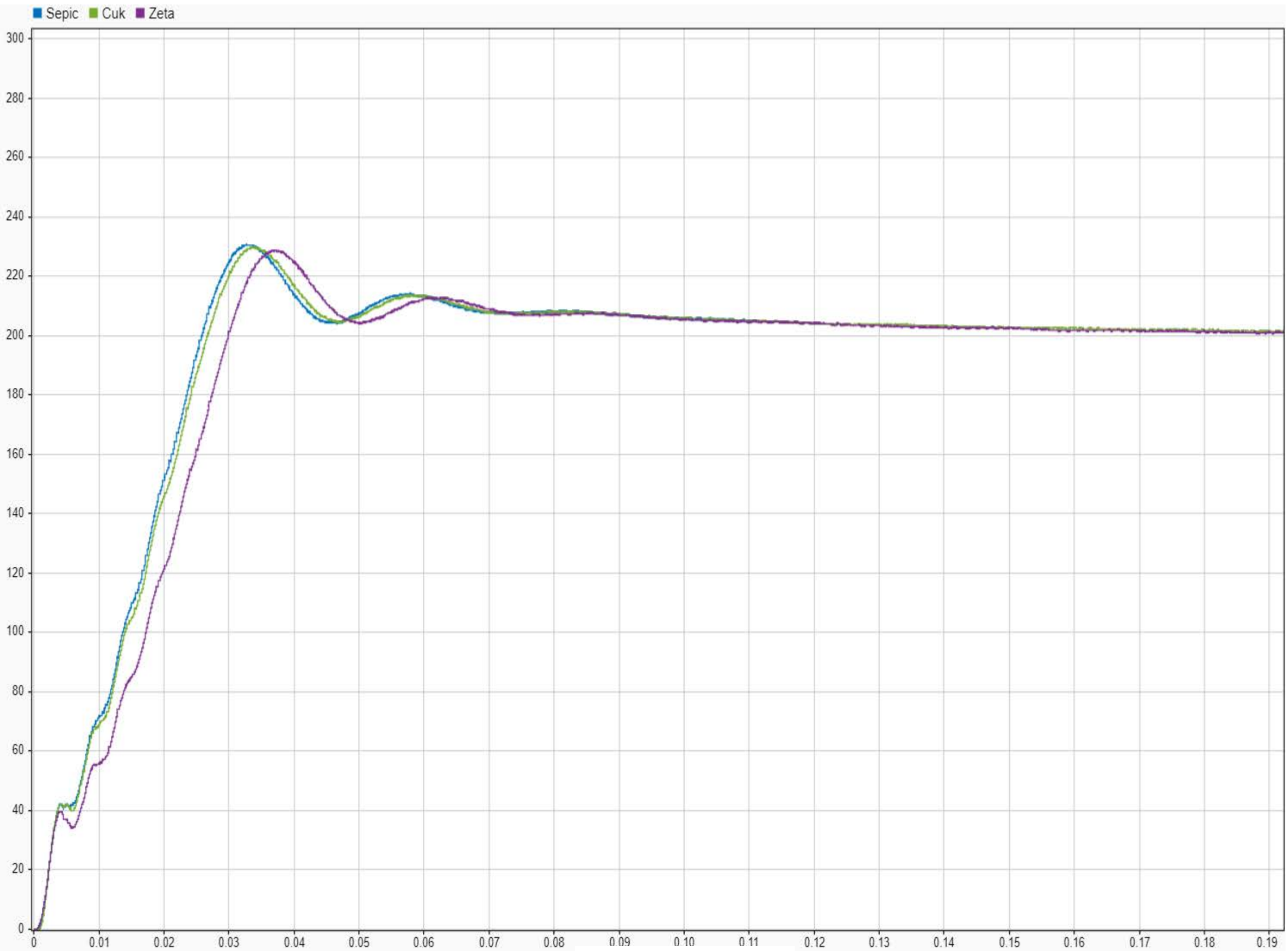

Fig. 24. DC link voltage characteristics of Zeta, Sepic and Cuk converters.

5.6. SVPWM SPEED CONTROL OF BLDC MOTOR

5.6.1. BLDC MOTOR OUTPUT CHARACTERISTICS FOR VARYING REFERENCE SPEED

Speed of BLDC motor is varied with reference starting from 3000RPM to 2500RPM to 2000RPM and BLDC motor characteristics at 9.1Mm load are shown in Fig. 25.

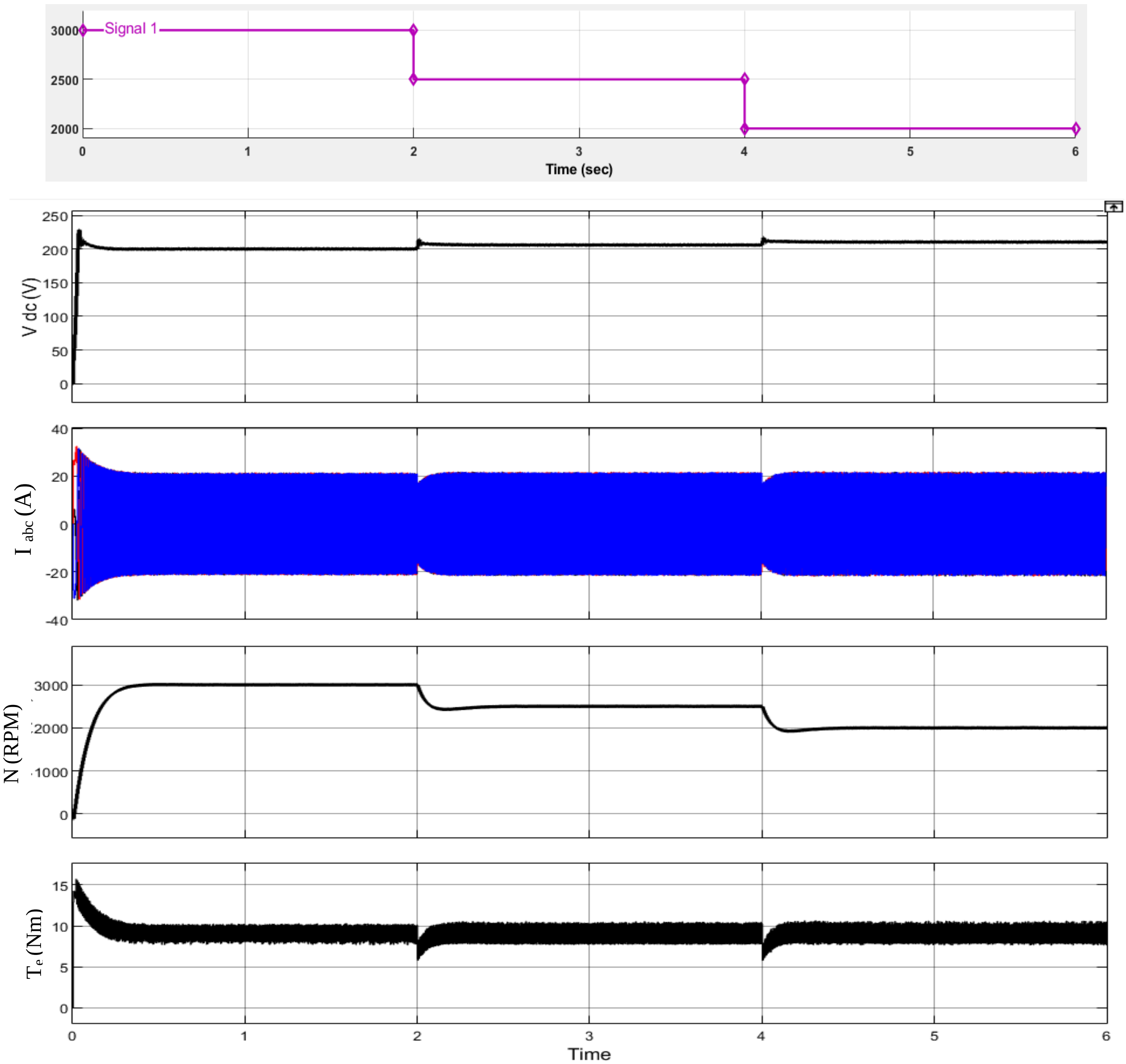

Fig. 25. BLDC motor output characteristics for reference speed variation.

5.6.2. SVPWM SPEED CONTROL TECHNIQUE PWM OUTPUT

SVPWM speed control output is given to inverter. The output is PWM signal for 3 phases of inverter which is generated for converter switches. The output waveforms are given in Fig. 26 which shows that the three waveforms are 120 degrees apart from each other.

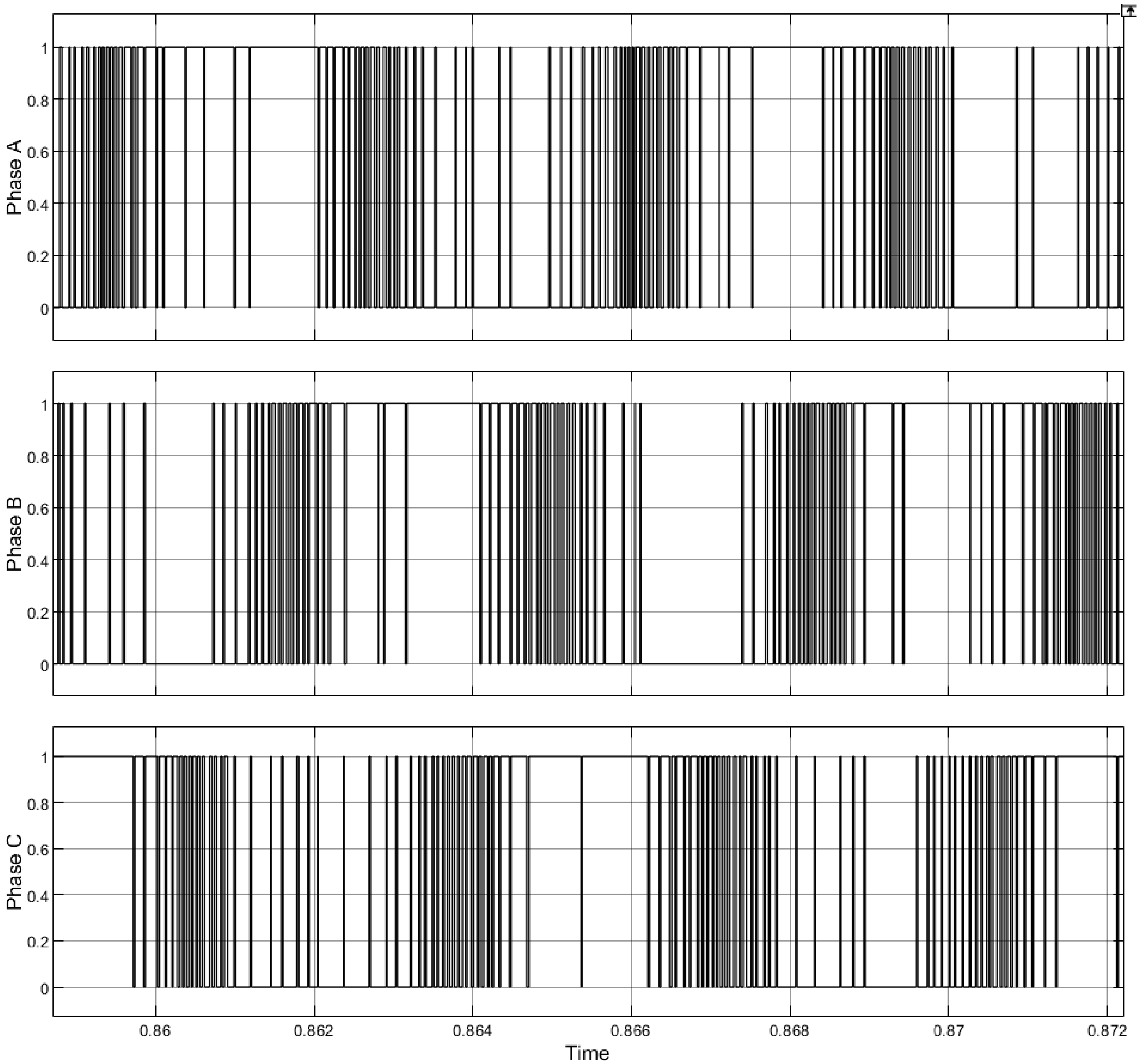

Fig. 26. SVPWM control technique output PWM signal.

CHAPTER 6: CONCLUSION AND FUTURE SCOPE OF WORK

6.1. CONCLUSION

The SPV array powered BLDC motor pump simulation has been designed successfully using Zeta, Sepic and Cuk converters. The BLDC motor speed and torque remain steady at rated value of 3000RPM and 9.1Nm during steady insolation of 1000W/m^2. MPPT module ensures operation of SPV array at 136V and 22.5A to ensure maximum power transfer. Testing of all the three converters with the complete simulation is performed with variation in insolation level where converter capacitor voltage stress was found to be least in Sepic converter which directly affects the voltage rating of capacitor to be used. Cuk converter showed maximum voltage stress across capacitor. However, during recovery period after insolation was set to 900W/m^2, Zeta converter input and output current as well as capacitor voltage waveforms show maximum ripples amongst three converters. Sepic converter performed best in recovery period also as no ripples are observed in the Sepic converter internal characteristics during recovery. Although the ripples in Zeta and Cuk converter does not affect the BLDC motor operation but these transient ripples are dangerous for converter components if not taken into consideration while designing. Thus, Sepic converter performance is found to be superior compared to Zeta and Cuk converter for BLDC motor equipped water pumping application using solar power.

6.2. FUTURE SCOPE OF WORK

Scope of future work in the solar water pumping system is diverse with respect to different versions of motors such as Switched reluctance motor and PMSM. Testing of new algorithms for implementation of MPPT is also to be explored.

REFERENCES

[1] Renewable energy vs Fossil fuels
https://www.inspirecleanenergy.com/blog/clean-energy-101/renewable-energy-vs-fossil-fuels

[2] Tata power solar
https://www.tatapowersolar.com/products/solar-water-pumps/

[3] Brushless DC Motors : Applications, Advantages and Controlling
https://www.eletimes.com/brushless-dc-motors-applications-advantages-and-controlling

[4] M. G. Villalva, J. R. Gazoli and E. R. Filho, "Comprehensive Approach to Modeling and Simulation of Photovoltaic Arrays," in IEEE Transactions on Power Electronics, vol. 24, no. 5, pp. 1198-1208, May 2009, doi: 10.1109/TPEL.2009.2013862.

[5] B. Tibor, V. Fedák and F. Durovský, "Modeling and simulation of the BLDC motor in MATLAB GUI," 2011 IEEE International Symposium on Industrial Electronics, 2011, pp. 1403-1407, doi: 10.1109/ISIE.2011.5984365.

[6] T. Esram and P. L. Chapman, "Comparison of Photovoltaic Array Maximum Power Point Tracking Techniques," in IEEE Transactions on Energy Conversion, vol. 22, no. 2, pp. 439-449, June 2007, doi: 10.1109/TEC.2006.874230.

[7] R. Kumar and B. Singh, "BLDC Motor-Driven Solar PV Array-Fed Water Pumping System Employing Zeta Converter," in IEEE Transactions on Industry Applications, vol. 52, no. 3, pp. 2315-2322, May-June 2016, doi: 10.1109/TIA.2016.2522943.

[8] A. K. Gupta and A. M. Khambadkone, "A Space Vector PWM Scheme for Multilevel Inverters Based on Two-Level Space Vector PWM," in IEEE Transactions on Industrial Electronics, vol. 53, no. 5, pp. 1631-1639, Oct. 2006, doi: 10.1109/TIE.2006.881989.

[9] Designing DC-DC converters based on Zeta Topology, https://www.ti.com/lit/an/slyt372/slyt372.pdf?ts=1627714810643&ref_url=https%253A%252F%252Fwww.google.com%252F

[10] Sepic converter design and operation https://web.wpi.edu/Pubs/E-project/Available/E-project-050114-131841/unrestricted/SEPIC_MQP_Final_Report.pdf

[11] Cuk Converter https://www.sciencedirect.com/topics/engineering/cuk-converter

[12] D. Sera, L. Mathe, T. Kerekes, S. V. Spataru and R. Teodorescu, "On the Perturb-and-Observe and Incremental Conductance MPPT Methods for PV Systems," in IEEE Journal of Photovoltaics, vol. 3, no. 3, pp. 1070-1078, July 2013, doi: 10.1109/JPHOTOV.2013.2261118.

[13] J. Rodriguez, Jih-Sheng Lai and Fang Zheng Peng, "Multilevel inverters: a survey of topologies, controls, and applications," in IEEE Transactions on Industrial Electronics, vol. 49, no. 4, pp. 724-738, Aug. 2002, doi: 10.1109/TIE.2002.801052.

[14] M. N. Gujjar and P. Kumar, "Comparative analysis of field oriented control of BLDC motor using SPWM and SVPWM techniques," 2017 2nd IEEE International Conference on Recent Trends in Electronics, Information & Communication Technology (RTEICT), 2017, pp. 924-929, doi: 10.1109/RTEICT.2017.8256733.

[15] One-Diode Model https://www.sciencedirect.com/topics/engineering/one-diode-model

[16] Y. Belkassmi, A. Rafiki, K. Gueraoui, L. Elmaimouni, O. Tata and N. Hassanain, "Modeling and simulation of photovoltaic module based on one diode model using Matlab/Simulink," 2017 International Conference on Engineering & MIS (ICEMIS), 2017, pp. 1-6, doi: 10.1109/ICEMIS.2017.8272965.

[17] R. Kumar and B. Singh, "BLDC Motor-Driven Solar PV Array-Fed Water Pumping System Employing Zeta Converter," in IEEE Transactions on Industry Applications, vol. 52, no. 3, pp. 2315-2322, May-June 2016, doi: 10.1109/TIA.2016.2522943.

[18] S. J. Chiang, H. Shieh and M. Chen, "Modeling and Control of PV Charger System With SEPIC Converter," in IEEE Transactions on Industrial Electronics, vol. 56, no. 11, pp. 4344-4353, Nov. 2009, doi: 10.1109/TIE.2008.2005144.

[19] A. Safari and S. Mekhilef, "Simulation and Hardware Implementation of Incremental Conductance MPPT With Direct Control Method Using Cuk Converter," in IEEE Transactions on Industrial Electronics, vol. 58, no. 4, pp. 1154-1161, April 2011, doi: 10.1109/TIE.2010.2048834.

[20] M. A. G. de Brito, L. Galotto, L. P. Sampaio, G. d. A. e Melo and C. A. Canesin, "Evaluation of the Main MPPT Techniques for Photovoltaic Applications," in IEEE Transactions on Industrial Electronics, vol. 60, no. 3, pp. 1156-1167, March 2013, doi: 10.1109/TIE.2012.2198036.

[21] B. Subudhi and R. Pradhan, "A Comparative Study on Maximum Power Point Tracking Techniques for Photovoltaic Power Systems," in IEEE Transactions on Sustainable Energy, vol. 4, no. 1, pp. 89-98, Jan. 2013, doi: 10.1109/TSTE.2012.2202294.

[22] D. Sera, T. Kerekes, R. Teodorescu and F. Blaabjerg, "Improved MPPT Algorithms for Rapidly Changing Environmental Conditions," 2006 12th International Power Electronics and Motion Control Conference, 2006, pp. 1614-1619, doi: 10.1109/EPEPEMC.2006.4778635.

[23] What is Space Vector Pulse Width Modulation (SVPWM) https://www.motioncontroltips.com/what-is-space-vector-pulse-width-modulation-svpwm/

[24] Space Vector PWM Techniques

https://encyclopedia.pub/109

[25] ADVANTAGES OF SPACE VECTOR MODULATION

https://www.electricalindia.in/advantages-of-space-vector-modulation/

APPENDIX

PARAMETERS OF SPV ARRAY

S. No.	Parameter	Value
1	V_{mpp}	136 V
2	V_m	22.7 V
3	I_{mpp}	23.55 A
4	I_m	11.83 A
5	P_{mpp}	3.2 kW
6	V_{oc}	27.2 V
7	I_{sc}	12.92 A
8	N_s	6
9	N_p	2

PARAMETERS OF BLDC MOTOR

S. No.	Parameter	Value
1	P	2.857 kW
2	N_r	3000 RPM
3	N_{min}	1500 RPM
4	T_m	9.1 Nm
5	V_{dc}	200 V
6	I_{dc}	16 A
7	N_p	6
8	J	1.75e-3
9	K_e	51
10	K_t	0.49
11	R_s	0.36 ohm
12	L_s	1.3e mH